OSU

The Ohio State University

USER'S MANUAL FOR SEMI-CIRCULAR COMPACT RANGE REFLECTOR CODE

by

Inder J. Gupta
Walter D. Burnside

The Ohio State University

ElectroScience Laboratory

Department of Electrical Engineering
Columbus, Ohio 43212

Technical Report 716148-11
Grant NSG 1613
April 1986

National Aeronautics and Space Administration
Langley Research Center
Hampton, Virginia 23665

NOTICES

When Government drawings, specifications, or other data are used for any purpose other than in connection with a definitely related Government procurement operation, the United States Government thereby incurs no responsibility nor any obligation whatsoever, and the fact that the Government may have formulated, furnished, or in any way supplied the said drawings, specifications, or other data, is not to be regarded by implication or otherwise as in any manner licensing the holder or any other person or corporation, or conveying any rights or permission to manufacture, use, or sell any patented invention that may in any way be related thereto.

50272-101

REPORT DOCUMENTATION PAGE	1. REPORT NO.	2.	3. Recipient's Accession No.

4. Title and Subtitle
User's Manual for Semi-Circular Compact Range Reflector Code

5. Report Date
April 1986

6.

7. Author(s)
Inder J. Gupta, Walter D. Burnside

8. Performing Organization Rept. No.
716148-11

9. Performing Organization Name and Address
The ElectroScience Laboratory
The Ohio State University
1320 Kinnear Road
Columbus, Ohio 43212

10. Project/Task/Work Unit No.

11. Contract(C) or Grant(G) No.
(C)
(G) NSG 1613

12. Sponsoring Organization Name and Address
National Aeronautics and Space Administration
Langley Research Center
Hampton, Virginia 23665

13. Type of Report & Period Covered
Technical

14.

15. Supplementary Notes

16. Abstract (Limit: 200 words)

A computer code has been developed at The Ohio State University ElectroScience Laboratory to analyze a semi-circular paraboloidal reflector antenna with a rolled edge at the top and a skirt at the bottom. The code can be used to compute the total near field of the antenna or its individual components at a given distance from the center of the paraboloid. Thus, it is very effective in computing the size of the 'sweet spot' for RCS or antenna measurement. This report describes the operation of the code. Various input and output statements are explained. Some results obtained using the computer code are presented to illustrate the code's capability as well as being samples of input/output sets.

17. Document Analysis a. Descriptors

b. Identifiers/Open-Ended Terms

c. COSATI Field/Group

18. Availability Statement
A. Approved for public release; distribution is unlimited.

19. Security Class (This Report)
Unclassified

21. No. of Pages
90

20. Security Class (This Page)
Unclassified

22. Price

(See ANSI-Z39.18) See Instructions on Reverse

OPTIONAL FORM 272 (4-77)
(Formerly NTIS-35)
Department of Commerce

TABLE OF CONTENTS

LIST OF TABLES

LIST OF FIGURES

I. INTRODUCTION

A computer code has been developed at The Ohio State University ElectroScience Laboratory to analyze a semi-circular paraboloidal reflector antenna with a rolled edge at the top and a skirt at the bottom as shown in Figure 1. The code can be used to compute the total near field of the antenna or its individual components at a given distance from the center of the paraboloid. The code computes the field along a radial cut (see Figure 1) at that distance. Thus, it is very effective in computing the size of the 'sweet spot' for a semi-circular compact range reflector. Various mechanisms included in the field computation are:

a) Specular reflection (geometrical optics term)

b) Junction diffraction (diffraction from the junction between the paraboloid and the rolled edge)

c) Skirt diffraction (diffraction from the junction between the lower end of the paraboloid and the skirt), and

d) Feed blockage.

The user has a choice of computing these mechanisms in any combination. The three field components (x,y,z) for each mechanism as well as the total field are stored in an output file.

This report describes the operation of the code. To help the user in understanding input data, a brief description of the method of

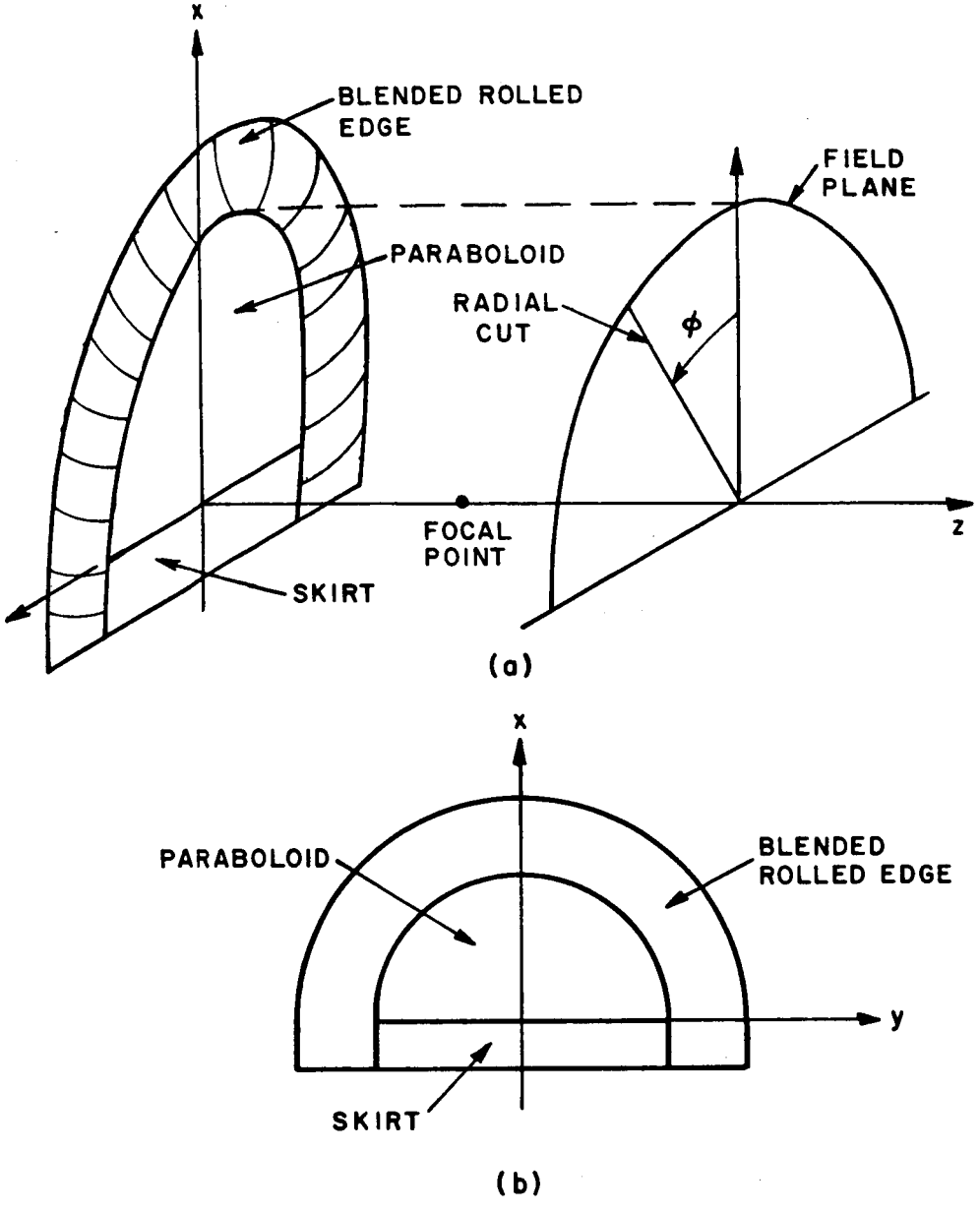

Figure 1(a). Paraboloid reflector with blended rolled edge at the top and skirt at the bottom and the field plane,

(b). Front view of the reflector.

computation of each mechanism is also given. Some results obtained using the computer code are presented to illustrate the code's capability as well as being samples of input/output sets.

A brief description of the methods of computation of the various mechanisms is given in the next section. Section III explains the input and output statements used in the code. Finally, Section IV contains various examples of the use of the code.

II. METHODS OF COMPUTATION

In this section, methods of computation of the various mechanisms included in the analysis of the reflector antenna are discussed. The purpose of this documentation is to help the user in understanding the input data. Various mechanisms included in the analysis are as follows:

A) Specular reflection

B) Junction diffraction

C) Skirt diffraction, and

D) Feed blockage.

A. SPECULAR REFLECTION

The code can be used to compute the specularly reflected field within a semicircular region at a given distance (along paraboloid axis) from the center of the paraboloid. The radius of the semicircle is equal to the radius of the paraboloid as shown in Figure 1. In this

region, the reflected field comes from the paraboloidal section of the reflector. Let (x_o,y_o,z_o) be the coordinates of the field point (observation point). Then, the reflected magnetic field is given by

$$\vec{H}^r(x_o,y_o,z_o) = \{\vec{H}^i(x_r,y_r,z_r) - 2\hat{n}\,[(\vec{H}^i(x_r,y_r,z_r)\cdot\hat{n})]\}\; e^{-jk(z_o-z_r)} \tag{1}$$

where (x_r,y_r,z_r) are the coordinates of the point of reflection. Note that $\vec{H}^i(x_r,y_r,z_r)$ is the incident magnetic field at that point, and $\hat{n}$ is the unit normal to the parabolic reflector at the point of reflection. In this case, one obtains

$$\begin{aligned} x_r &= x_o \\ y_r &= y_o \\ \text{and } z_r &= (x_o^2 + y_o^2)/4F \end{aligned} \tag{2}$$

where F is the focal distance of the paraboloid. Thus, knowing the feed pattern and the coordinate of the observation point, the reflected field can be computed.

B. SKIRT DIFFRACTION

The diffracted field from the junction between the lower end of the paraboloid and the skirt is computed using the Geometrical Theory of Diffraction. The GTD diffraction coefficients [1] are used to compute the diffracted field. Since this is a smooth junction, the diffracted field will be due to the discontinuity in the reflected field.

The diffracted field from a smooth junction (see Figure 2) is given by [2]

$$\begin{bmatrix} E_\beta^d \\ E_\phi^d \end{bmatrix} = \begin{bmatrix} -D_s & 0 \\ 0 & -D_h \end{bmatrix} \begin{bmatrix} E_{\beta'}^i \\ E_{\phi'}^i \end{bmatrix} \sqrt{\frac{\rho}{(s+\rho)s}}\, e^{-jks} \tag{3}$$

where

$$D_{\substack{s \\ h}}(\phi,\phi',\beta_o) = \pm \frac{e^{-j\pi/4}}{2\sqrt{2\pi k}\,\sin\beta_o} \tan\left(\frac{\phi+\phi'}{2}\right) \cdot$$

$$\{F[kL^{r_o} a(\phi+\phi')] - F[kL^{r_n} a(\phi+\phi')]\} \tag{4}$$

$$L^{r_o} = \frac{s(\rho_e^r+s)\,\rho_1^{r_o}\,\rho_2^{r_o}}{\rho_e^r(\rho_1^{r_o}+s)(\rho_2^{r_o}+s)} \sin^2\beta_o \tag{5}$$

$$L^{r_n} = \frac{s(\rho_e^r+s)\rho_1^{r_n}\,\rho_2^{r_n}}{\rho_e^r(\rho_1^{r_n}+s)(\rho_2^{r_n}+s)} \sin^2\beta_o \tag{6}$$

$$a(\phi+\phi') = 2\cos^2\left(\frac{\phi+\phi'}{2}\right) \tag{7}$$

$$\frac{1}{\rho_e^r} = \frac{1}{\rho_e^i} - \frac{2(\hat{n}\cdot\hat{n}_e)(\hat{s}'\cdot\hat{n})}{a_e \sin^2\beta_o} \tag{8}$$

$$\frac{1}{\rho} = \frac{1}{\rho_e^i} - \frac{\hat{n}_e\cdot(\hat{s}'-\hat{s})}{a_e \sin^2\beta_o} \tag{9}$$

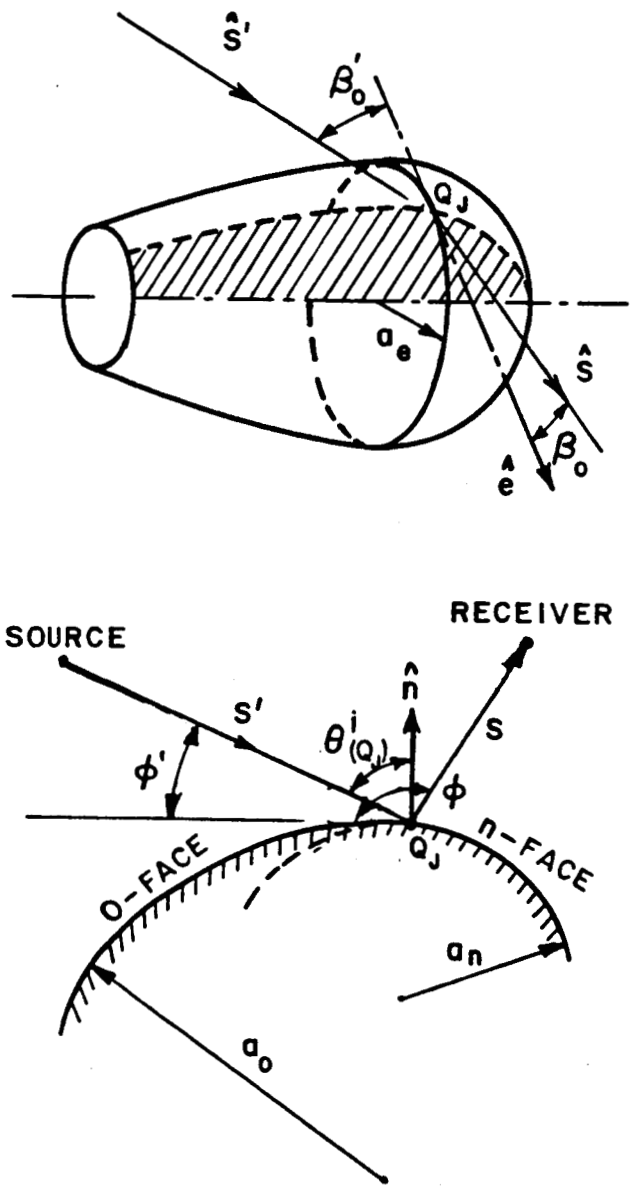

Figure 2. A 3-dimensional wedge with smooth junction.

$$\frac{1}{\rho_1^{r_{o,n}}} = \frac{1}{\rho_1^i} + \frac{2}{a_e \cos\theta_i}, \text{ and} \tag{10}$$

$$\frac{1}{\rho_2^{r_{o,n}}} = \frac{1}{\rho_2^i} + \frac{2\cos\theta_i}{a_{o,n}} . \tag{11}$$

The various parameters used in Equations (3) - (11) are defined as follows:

ρ_1^i, ρ_1^r = the principal radii of curvature of the (incident, reflected) wavefront at Q_J in the plane of incidence

ρ_2^i, ρ_2^r = the principal radii of curvature of the (incident, reflected) wavefront at Q_J in the transverse plane

a_e = the radius of curvature of the edge at Q_J

$\hat{n}$ = the unit normal to the surface at Q_J

$\hat{n}_e$ = the unit normal to the edge at Q_J directed away from the center of edge curvature

$\hat{s}'$ = the unit vector in the incident ray direction at Q_J

$\hat{s}$ = the unit vector in the diffracted ray direction at Q_J

$\hat{e}$ = the unit tangent to the edge at Q_J

β_o = the angle between the incident and edge tangent directions such that

$$\cos\beta_o = \hat{e} \cdot \hat{s}' \tag{12}$$

$\hat{\phi}', \hat{\phi}$ = the unit vectors in the plane perpendicular to the edge at Q_J

$$\hat{\beta}' = \hat{s}' \times \hat{\phi}' \tag{13}$$

$$\hat{\beta} = \hat{s} \times \hat{\phi} \tag{14}$$

and

ρ_e^i = the radius of curvature of the incident wavefront at Q_J in the plane containing $\hat{e}$ and $\hat{s}'$.

For the paraboloid-skirt junction, assuming the skirt to be the 0-face and the feed is at the focus, one obtains

$$\rho_e^r = \rho_1^{r_{o,n}} = \infty$$

$$\rho_2^{r_n} = \infty, \text{ and} \tag{15}$$

$$\rho_2^{r_o} = \rho_2^i \quad .$$

Thus, the distance parameters are given by

$$L^{r_o} = \frac{s\rho_2^{r_o}}{(\rho_2^{r_o}+s)} \sin^2\beta_o, \text{ and} \tag{16}$$

$$L^{r_n} = s \quad . \tag{17}$$

Knowing the coordinates of the observation point (x_o, y_o, z_o), one can find the point of diffraction on the edge. The law of diffraction will be satisfied at the point of diffraction. Once the point of diffraction is found, one can compute the incident field $(E^i_{\beta'}, E^i_{\phi'})$ at that point. The angles (β_o, ϕ and ϕ') can also be found. Knowing ρ^i_1 and ρ^i_2, one can compute ρ, L^{r_o}, L^{r_n} and then using (3), the diffracted fields can be calculated. Note that $\phi' = 90°$ in this case.

C. JUNCTION DIFFRACTION

The junction between the paraboloid and rolled edge is a higher order discontinuity in that at least the slope is continuous. For the blended rolled edge, the junction is continuous to even higher order derivatives. Since GTD diffraction coefficients for these higher order discontinuities are not available, a new technique has been developed to find the diffracted field from the junction. In this new technique, the first step is to reduce the three-dimensional problem to a two-dimensional one; i.e., the reflector is replaced by an infinitely long cylinder of the same cross section as that of a radial cut through the reflector as shown in Figure 3(a). This radial cut contains the point of diffraction. The skirt part of this cylinder is then replaced with a parabolic cylinder with the same focal length as the paraboloidal section. A cross section view of the cylinder is shown in Figure 3(b). Note that the cross section of the cylinder is independent of which radial cut is taken in that the reflector has rotational symmetry. The total field scattered by this cylindrical reflector with a rolled edge

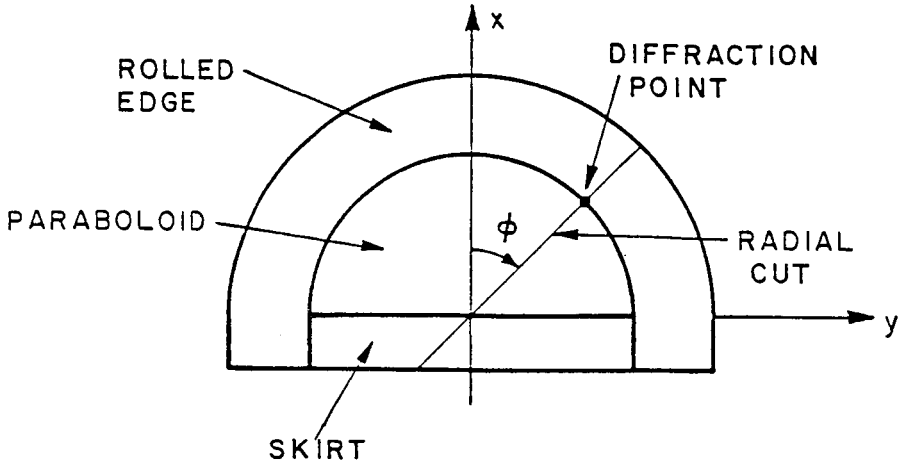

(a)

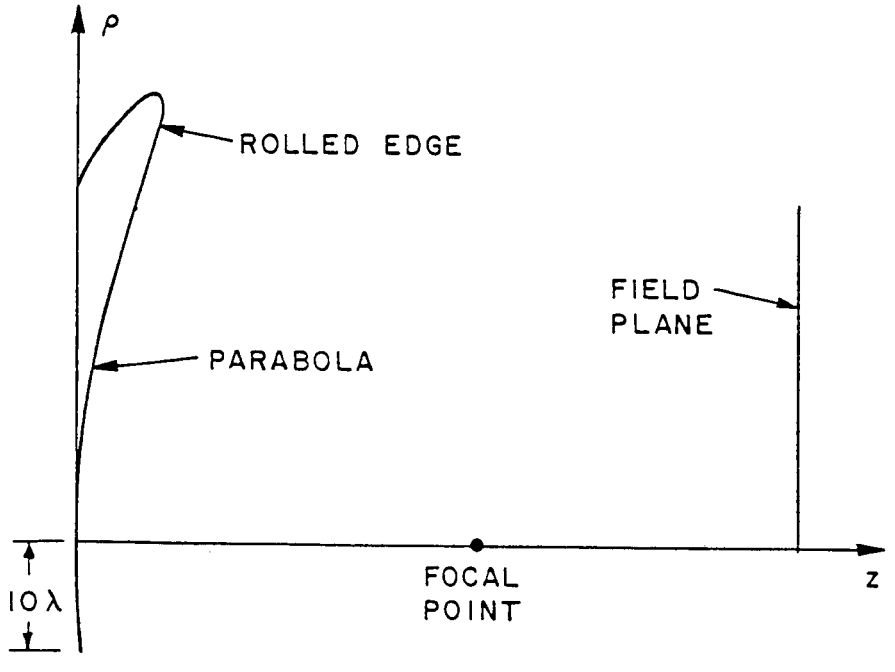

(b)

Figure 3(a). Radial cut on the paraboloid reflector.

(b). Cross-sectional view of the infinite cylinder.

is found using physical optics. Since it is a two-dimensional problem, one has to do a contour integration to compute the total field. Thus, physical optics integration can be carried out quite efficiently. The total field obtained using the PO integration contains contributions from four different mechanisms as shown in Figure 4(a). These mechanisms are as follows:

1. Stationary point contribution (specular reflected field)
2. Two end point contributions, and
3. Diffracted field from the junction.

The stationary point contribution and the end point contributions from the cylinder are known. For example, assuming that the cylinder is illuminated by a magnetic line source (see Figure 4(b)), the PO scattered magnetic field is given by

$$\vec{H}^s = c \int_o^{\ell} (\vec{J}_{po} \times \hat{s}) \frac{e^{-jks}}{\sqrt{s}} d\ell \qquad (18)$$

where c is a constant, $\hat{s}$ is the unit vector in the observation direction, and $\vec{J}_{po}$ is the physical optics current which is given by

$$\vec{J}_{po} = 2 \hat{n} \times \vec{H}^i \quad . \qquad (19)$$

The ϕ component of $\vec{H}^s$ is

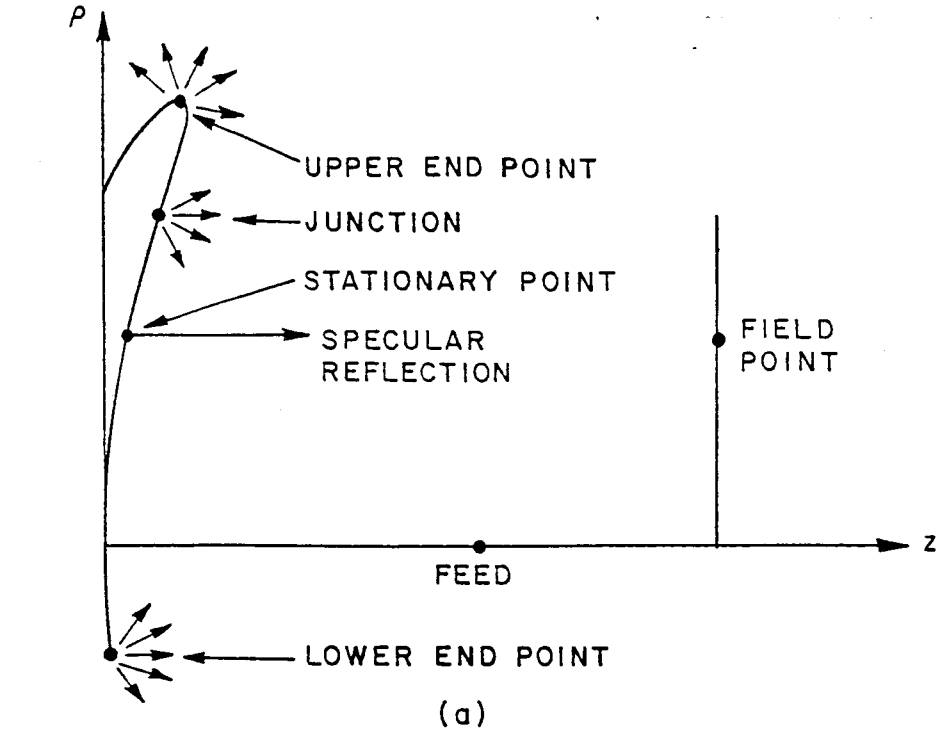

(a)

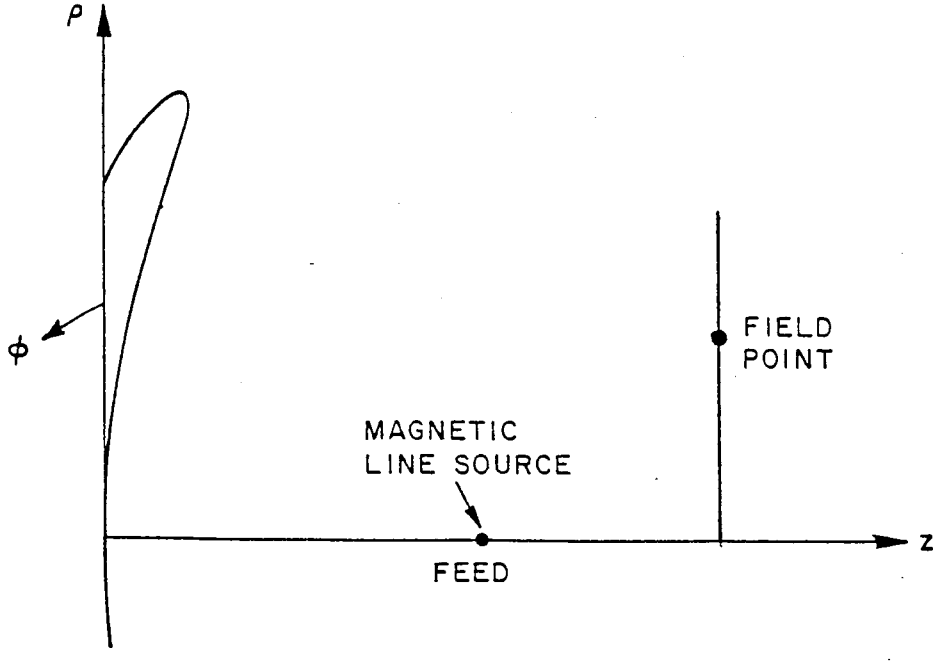

(b)

Figure 4(a). Various mechanisms contributing to the scattered field.

(b). Magnetic line source illumination of an infinitely long cylinder.

$$H_\phi^s = c \int_0^\ell \hat{\phi} \cdot (\vec{J}_{po} \times \hat{s}) \frac{e^{-jks}}{\sqrt{s}} \, d\ell = c \int_0^\ell F \, e^{jk\Phi} \, d\ell \tag{20}$$

where

$$\frac{\hat{\phi} \cdot (\vec{J}_{po} \times \hat{s})}{\sqrt{s}} = F \, e^{jk\tilde{\Phi}} \tag{21}$$

$$\text{and } \Phi = \tilde{\Phi} - s \tag{22}$$

Then the end point contributions are each given by

$$H_\phi^e = c \sum_{n=0}^{\infty} \frac{(-1)^n F_n}{jk\Phi'} \, e^{-jk\Phi} \Bigg|_0^\ell \tag{23}$$

$$\text{where } F_n = \frac{d}{d\ell} \frac{F_{n-1}}{jk\Phi'} \tag{24}$$

$$\text{and } F_0 = F. \tag{25}$$

The first two terms of the infinite series give a good approximation to the end point contribution. In (23), the end points are assumed to be far from the stationary point. This condition is easily met by the upper end point. However, the same may not be true for the lower end point. To meet this requirement, the skirt should be replaced by a parabolic section of dimension at least 10 wavelengths as shown in Figure 4(b). The focal length of the parabolic section is equal to that of the original reflector.

The stationary point contribution and the end point contributions are subtracted from the PO scattered field. This leaves the diffracted field which comes from the junction between the parabola and the rolled edge. This is a two-dimensional diffracted field, which means that an appropriate spread factor must be applied to this field in order to obtain the desired three-dimensional diffracted field. One needs the coordinates of the junction to find the spread factor. This is an input parameter and is equal to the radius of the paraboloidal section of the reflector.

One also needs to input the cross sectional shape of the cylinder to carry out the physical optics integration. This geometrical shape is read from unit #17. The data file linked to unit #17 has the following information:

1. Number of samples (NS) along the cross section
2. ρ and z coordinates of the various samples in centimeters

This file is read using the following formats:

```
      Read (17,*) NS
      Do 2 I=1, NS
 2    Read (17,*) (Z(I),ρ(I)).
```

Note that the "*" symbol indicates free format input. The spacing between the samples should be of the order of 0.05λ, where λ is the wavelengths in centimeters. As written, the code can handle a maximum of 2001 samples ($NS \leq 2001$). If the number of samples exceeds this value, the first statement in the code should be changed accordingly.

D. FEED BLOCKAGE

The feed blockage is computed using a physical optics integration technique. The feed aperture is assumed to be a flat plate located at a distance Z_a from the center of the paraboloid. The flat plate is defined by the coordinates of its corners. The number of corners and their coordinates are input parameters. The plate is assumed to be symmetrical about the x_a axis as shown in Figure 5. The field incident on the flat plate is assumed to be uniform and equal to the specular reflected field at $(0,0,Z_a)$. For small plates, the surface integration is replaced by a contour integration along the periphery of the plate [3]. For large plates, the plate is subdivided into rectangular patches as shown in Figure 5(b). As written, the maximum number of rectangular segments is equal to 625. The corners of the flat plate are numbered in a clockwise fashion as shown in Figure 5(b).

The various input and output statements are explained in the next section.

III. INPUT AND OUTPUT STATEMENTS

A. INPUT DATA

The code is written to accept the input data on an interactive basis in free format, i.e., a statement will appear on the user's terminal explaining what input is needed. These statements are self explanatory and can be divided into two groups as follows:

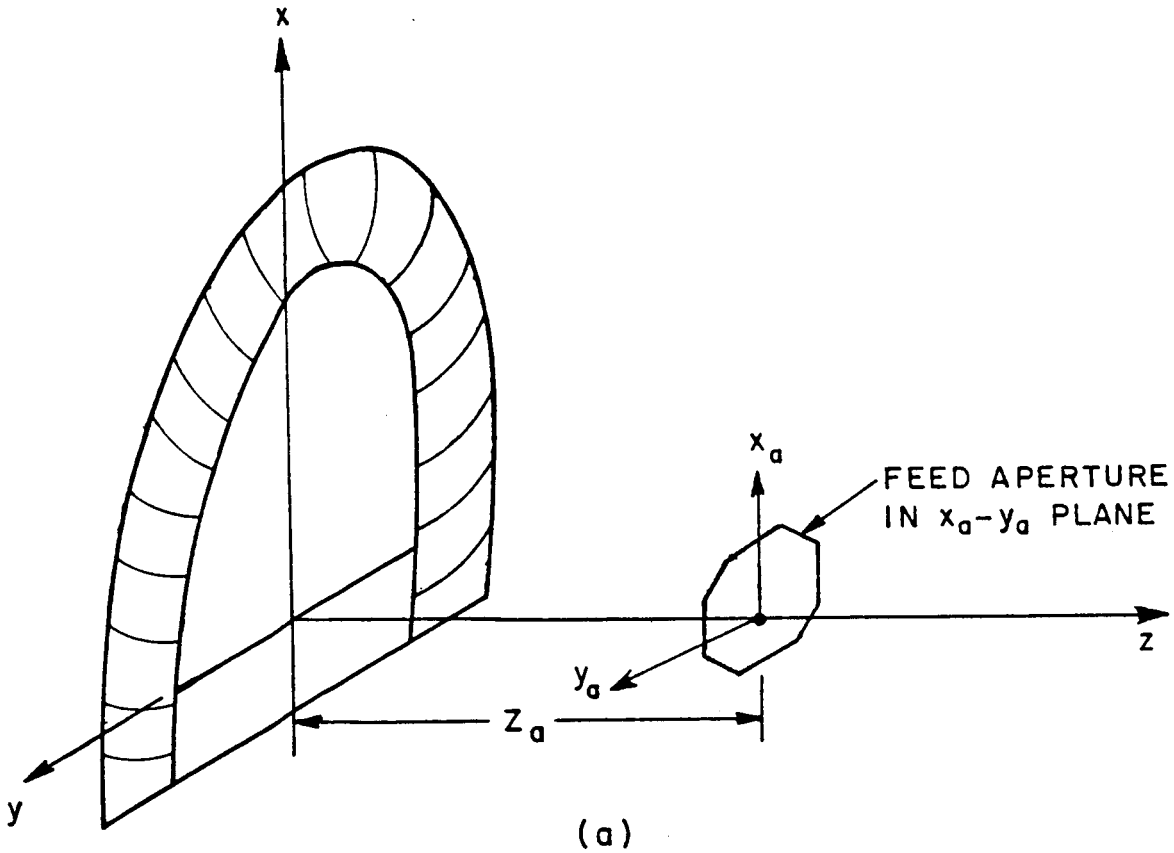

(a)

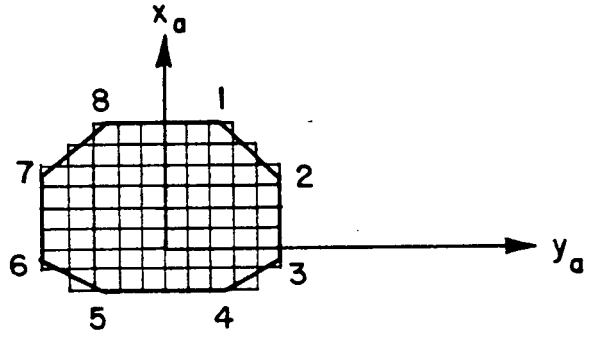

(b)

Figure 5. Flat plate used to compute feed blockage. The plate is symmetrical about the x_a axis. Note that the x_a-y_a plane is parallel to the x-y plane.

a) General input data, and

b) Specific input data.

General input data is needed to compute any one of the four mechanisms. Specific input data is the input for an individual mechanism. General input data consists of the following statements:

1. Input the frequency in GHz.
2. Input the distance of the focal point from the center of the paraboloid in feet.
3. Input the tilt angle of the feed.
4. Input the magnitude of the magnetic dipoles along x and y axes.
5. Input the magnitude of the electric dipoles along x and y axes.
6. Input the distance of the field plane from the center of the paraboloid in feet.
7. Input the phi cut in degrees.
8. Input the start point and end point for probing.
9. Input the distance between field points in feet.
10. Do you want GO term? If yes, type 1.
11. Do you want junction diffraction? If yes, type 1.
12. Do you want skirt diffraction? If yes, type 1.
13. Do you want feed blockage? If yes, type 1.
14. Do you want electric field components? If yes, type 1.

Statements 1 and 2 define the frequency of operation and the focal length of the paraboloid. Statements 3, 4 and 5 define the feed configuration. The phase center of the feed is assumed to be at the focus of the reflector (see Figure 1). The feed may be tilted as shown in Figure 6. The tilt angle (α) is defined in statement 3. The feed is simulated using four short dipoles (two magnetic dipoles and two electric dipoles). Two dipoles are oriented along X_f (if dipoles are oriented along negative X_f, the magnitude of the dipoles will be negative) and the other two are oriented along y_f. The dipole magnitudes are their magnetic field strength at a unit distance. For example, for a magnetic dipole oriented as shown in Figure 7, the magnetic field is given by

$$\vec{H} = -\hat{\theta}\, H_m \sin\theta \frac{e^{-jkR}}{R} \tag{26}$$

where H_m is input to the program and R is the distance of the observation point from the dipole in centimeters. Similarly, for an electric dipole oriented along the z axis, the magnetic field is given by

$$\vec{H} = -\hat{\phi}\, H_e \sin\theta \frac{e^{-jkR}}{R} \tag{27}$$

where H_e is the input to the program. The magnitudes of the various dipoles are defined in statements 4 and 5.

Statements 6, 7, 8 and 9 define the probing distance, phi cut and the length which is to be probed. Various parameters to be defined with

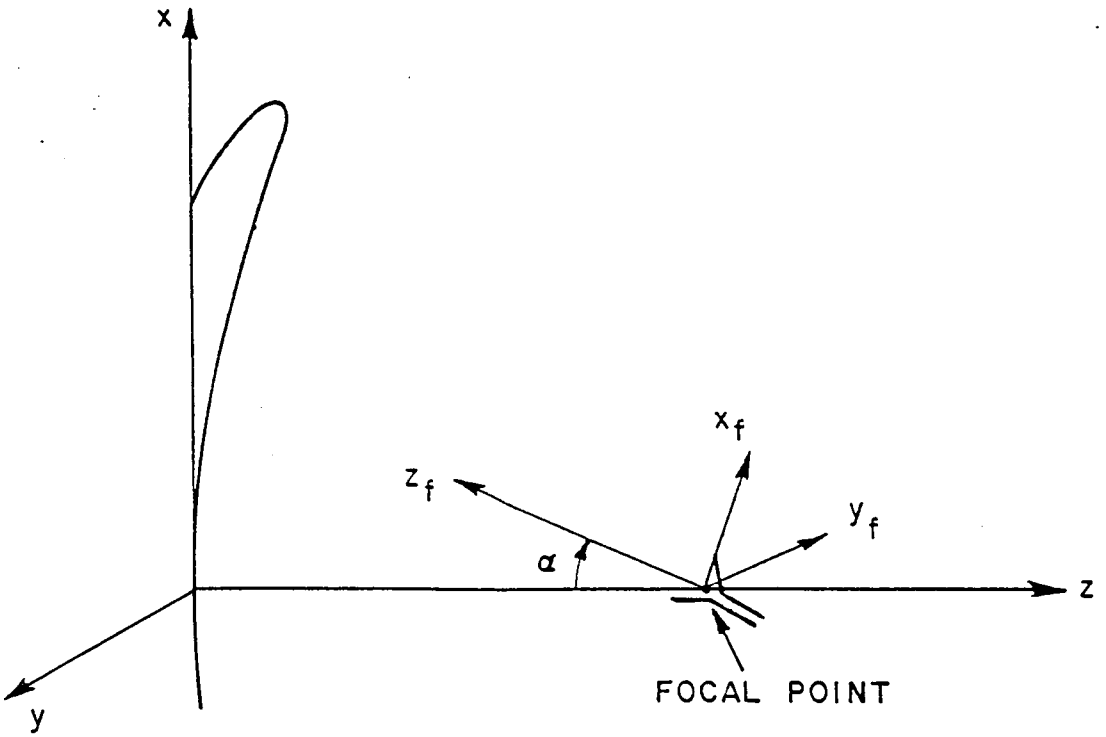

Figure 6. Feed configuration with feed tilt specified by α.

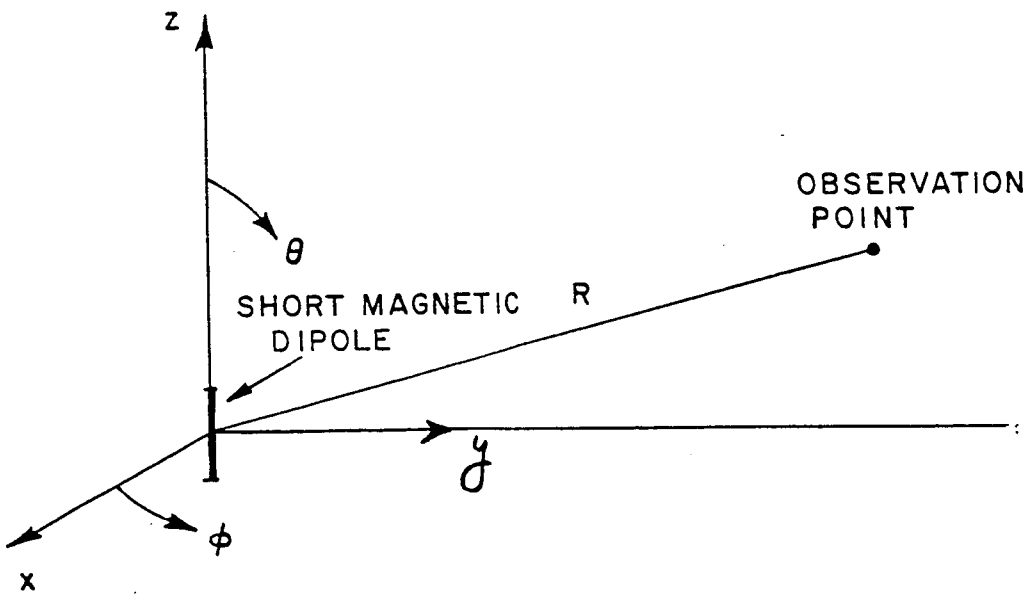

Figure 7. Short magnetic dipole.

these statements are shown in Figure 8. Note that Z_0 in this figure is the distance of the field plane from the center of the paraboloid. The angle (ϕ) is the phi cut for field probing which is limited between 0° and 90°. The performance for $\phi<0°$ will be the same as for $\phi>0°$. The start and end points for probing are also shown in the figure. Note that for a semicircular field plane, the start and end points are independent of the phi cut (ϕ). The start and end points should lie between 0 and R, where R is equal to the radius of the paraboloid. The distance between field points should be chosen such that the total number of field points is at least equal to 75. Presently, the code is set to compute the field at a maximum of 201 points. If more than 201 points are needed, one should change statement 2 in the code accordingly.

Statements 10, 11, 12 and 13 define the various mechanisms to be computed. One can choose any combination of mechanisms. Specific data for each mechanism is discussed below.

Statement 14 defines the output. The code computes both electric and magnetic fields but only one is stored as an output file. The output field chosen by the user is defined by statement 14.

Specific input data for the various mechanisms is defined as follows:

i) **Specular Reflection (GO):** No specific input required.

ii) **Junction Diffraction:** To compute junction diffraction, as discussed in Section II, one should define the distance of the junction from the center of the paraboloid. This is equal to the radius of the

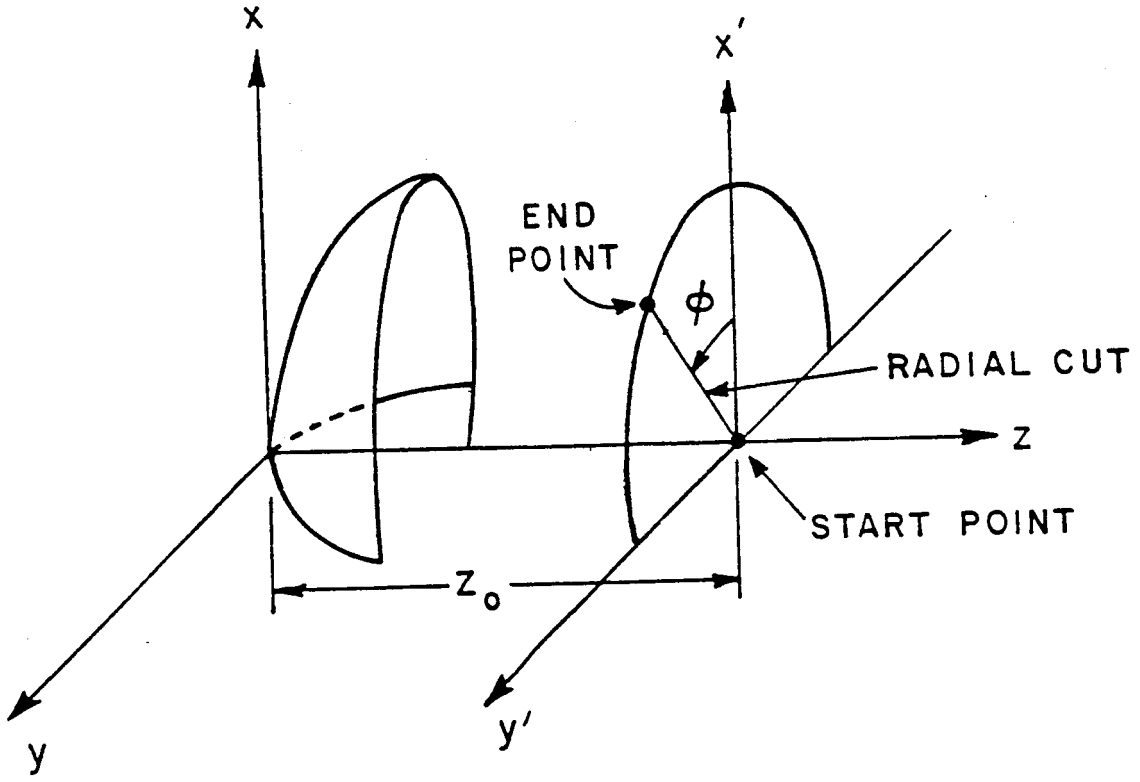

Figure 8. Description of the observation plane.

paraboloidal section of the reflector. The following statement will appear on the user's terminal.

'Input the distance of the junction from the center of the paraboloid in feet'.

In addition, one needs to input the cross-section of the cylinder (see Section II) for the physical optics integration. This information should be input on unit #17 and is automatically read by the code. The format of this input data was given in Section II.

iii) **Skirt Diffraction:** No specific input required.

iv) **Feed Blockage:** To compute the feed blockage, the feed aperture is assumed to be a flat plate whose normal is aligned with the z axis of the original reflector system. The flat plate is defined by the coordinates of its corners. If the feed aperture is circular, it should be approximated by a polygon. The geometry of the flat plate is read by the following input statements.

1. Input the z location of the feed aperture in feet.
2. Input the number of corners in the feed aperture.
3. Input the x,y coordinates of the corners in inches.

The z location of the feed aperture is the distance along the z axis from the center of the paraboloid. Statement 2 defines the number of corners in the flat plate. As written, the maximum number of corners permitted in the code is ten. Statement 3 defines the coordinates of the corners of the plate. As discussed in Section II, the corners are numbered according to a clockwise convention with the first corner along the positive x direction or in the first quadrant with the smallest distance from the x axis. The plate is assumed to be symmetrical about the x axis.

B. OUTPUT DATA

The code stores the field due to each mechanism as well as the total field in terms of separate output files. As chosen by the user, all three components (x,y,z) of either the electric or the magnetic field are stored. The specular reflected field is stored on unit #20, the junction diffraction on unit #21, the skirt diffraction on unit #22, the feed blockage on unit #23, and the total field on unit #24. The fields are stored for various radial distances from the paraboloid axis using the following format:

```
      WRITE (IUNIT,100) DIS(I), FX(I), FY(I), FZ(I)
100   FORMAT (7E 16.6)
```

where IUNIT=20, 21, 22, 23 or 24; FX(I), FY(I) AND FZ(I) are the x,y, and z components of the field at I^{th} probing point and DIS(I) is the radial distance (in feet) of the I^{th} probing point.

Some sample results obtained using this code are given in the next Section.

IV. SAMPLE RESULTS

In this section, some results obtained using the computer code are presented to illustrate the code's capability as well as being samples of input/output sets. Scientific-Atlanta's 15 foot reflector antenna with a blended rolled edge is used for illustration. The focal length of the reflector is 24 feet, and the frequency of operation is 2 GHz. Figure 9 shows a cross-sectional view (in the xz plane) of the reflector. Note that the reflector has a blended rolled edge at the top

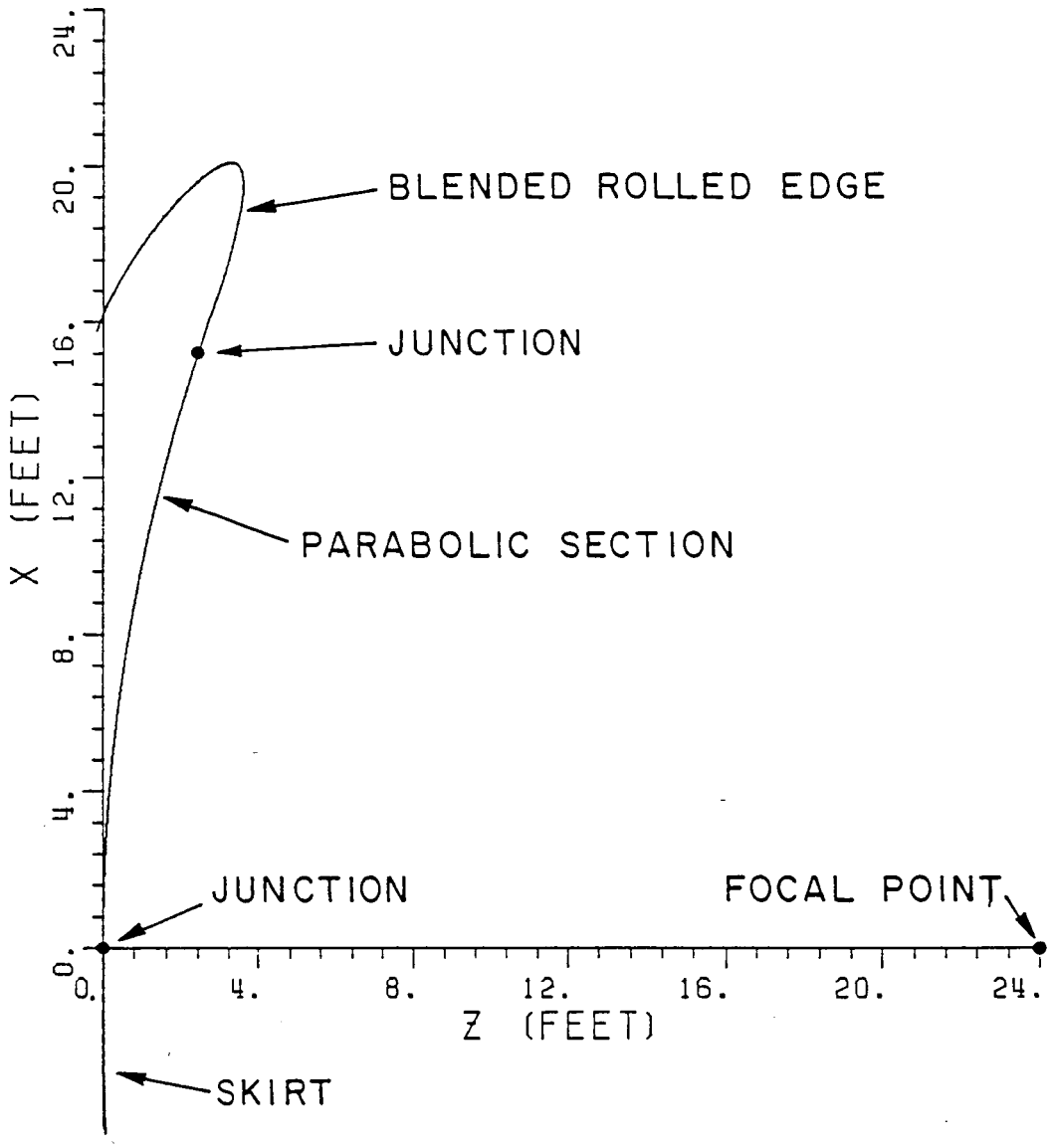

Figure 9. Cross-sectional view of the semi-circular Scientific-Atlanta reflector in the xz plane.

and a skirt at the bottom. The semi major axis of the elliptical section used as the rolled edge is 100 centimeters (cm) and its semi minor axis is 40 cm. The length of the parabolic section used in the blended rolled edge is 400 cm. The two sections (elliptical and parabolic) are blended using a cosine blending function [see Appendix A].

The code is used to compute the field scattered by the reflector along various radial cuts at a distance of 36 feet from the center of the reflector. The total scattered field as well as field scattered in terms of the individual mechanisms are computed. As pointed out in Section II, one needs the cross-sectional shape of the infinitly long cylinder to compute the diffraction from the junction between the paraboloid and the blended rolled edge. This cross-sectional shape was obtained using the computer code "SURFACE". A listing of the computer code "SURFACE" is given in Appendix A. This code reads the input data from unit #70. The input data file assigned to unit #70 contained the following information:

```
2.
24.
15.
-5.
4
400.
180.
100., 40.
0.05
```

Figure 10 shows the cross-sectional shape obtained using the computer code. Note that the cross-sectional shape is similar to the cross-section of the reflector (see Figure 9) except that the skirt is replaced by a parabolic section. The length of the parabolic section is 5 feet which is roughly equal to 10 wavelengths at 2 GHz. The scattered field along a vertical cut (ϕ=0°) for various feeds is computed first. The scattered magnetic field is plotted here.

Figure 11 shows the co-polarized (y) component† of the scattered magnetic field in a vertical cut (ϕ=0°) at a distance of 36 feet from the center of the reflector when the feed is a short magnetic dipole oriented along y_f axis (see Figure 6). The tilt angle of the feed is zero. The various mechanisms included in the field computation are the specular reflection, junction diffraction and skirt diffraction. The plot in Figure 11 was obtained by using the output on unit #24. The input data to the code is given below which was input on an interactive basis:

```
 INPUT THE FREQUENCY IN GHz.
2
 INPUT THE DISTANCE OF THE FOCAL POINT FROM THE
 CENTER OF THE PARAPOLOID IN FEET
24.
 INPUT THE TILT ANGLE OF THE FEED
0.
 INPUT THE MAGNITUDE OF THE MAGNETIC DIPOLES
 ALONG X AND Y AXES
0.,1.
 INPUT THE MAGNITUDE OF THE ELECTRIC DIPOLES
 ALONG X AND Y AXES
0.,0.
```

---

† The cross-polarized component (x component) in this case is negligible.

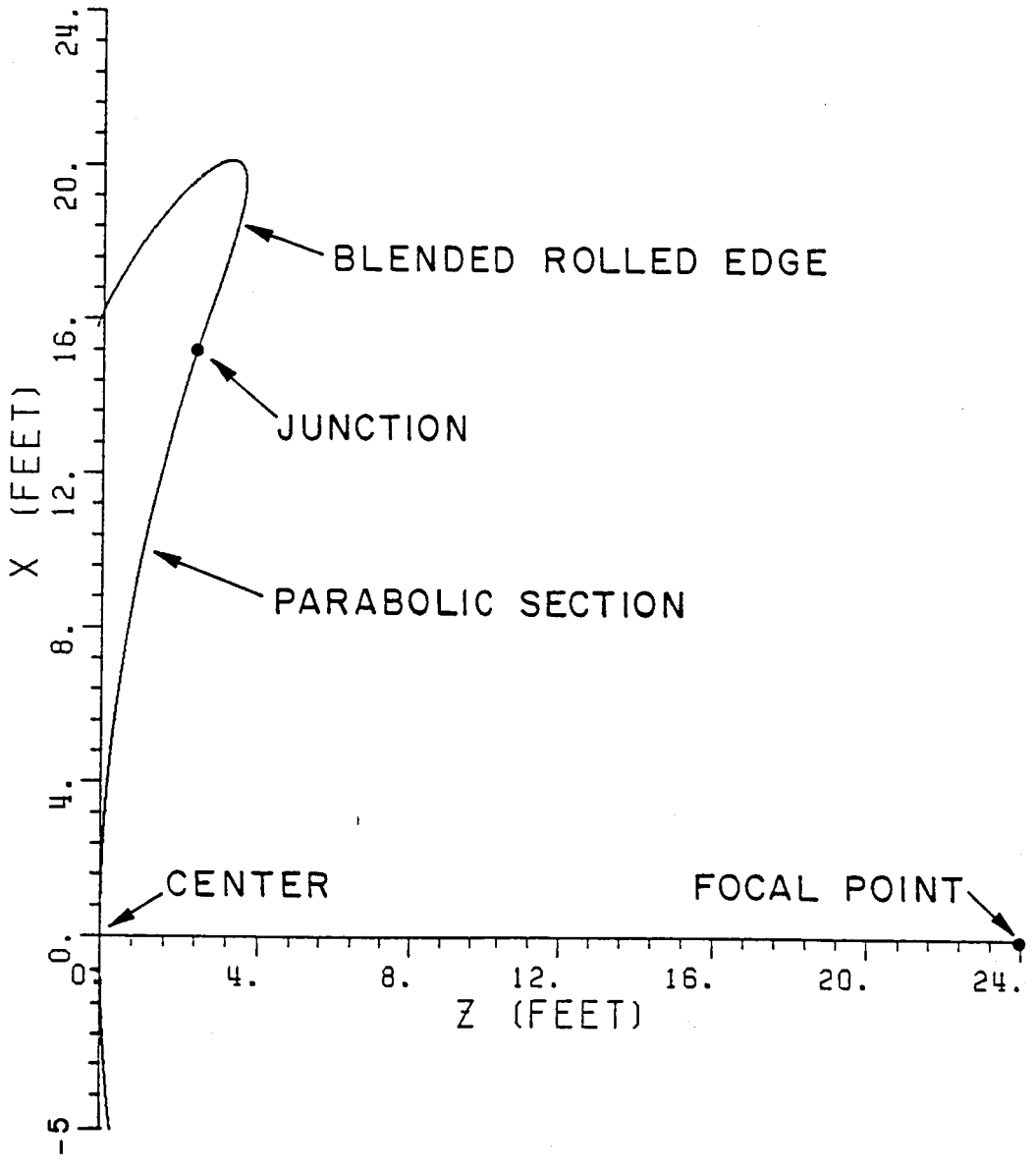

Figure 10. Cross-sectional shape of the infinitely long cylinder.

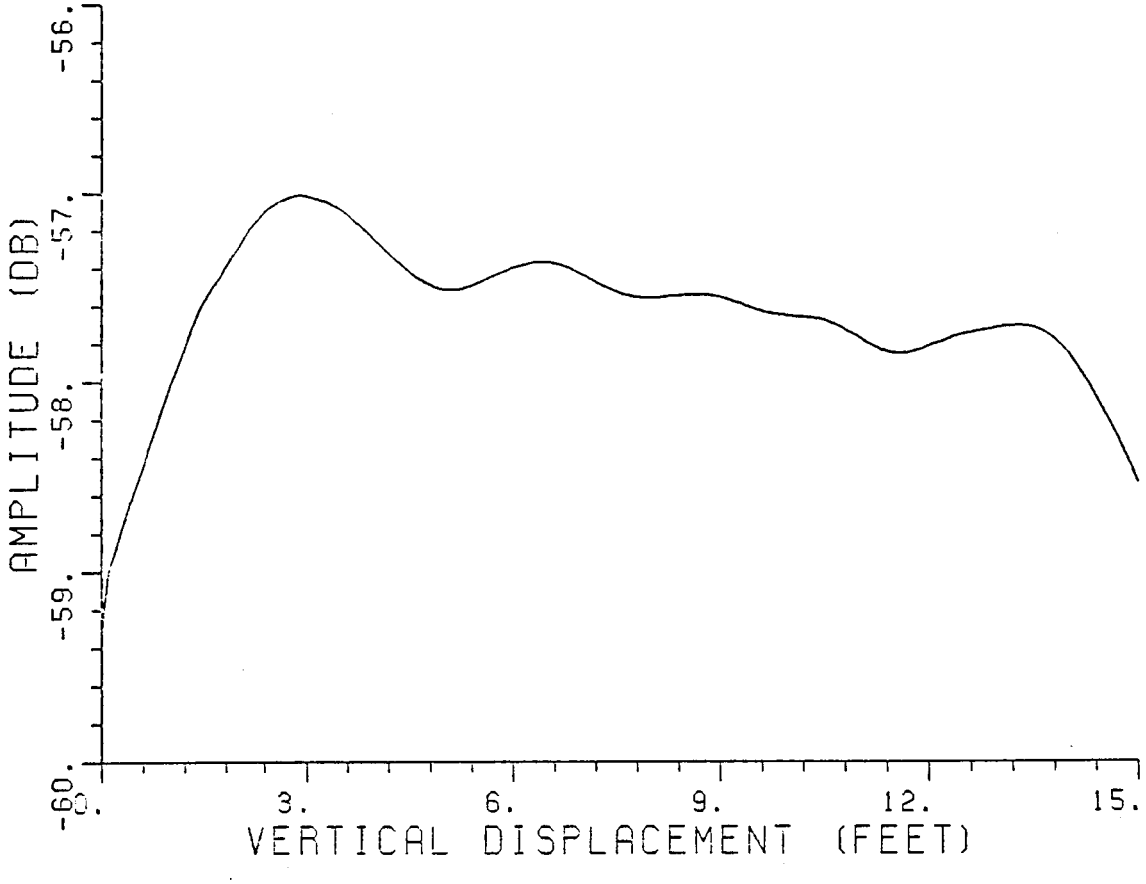

Figure 11. The co-polarized (y) component of the scattered magnetic field versus vertical displacement. Note that $\phi=0°$, and feed is a short horizontal magnetic dipole. Various mechanisms included in the scattered field are:

1. specular reflection
2. junction diffraction
3. skirt diffraction

```
 INPUT THE DISTANCE OF THE FIELD PLANE FROM THE CENTER
 OF THE PARABOLOID IN FEET
36.
 INPUT THE PHI CUT IN DEGREES
0.
 INPUT START POINT AND END POINT FOR FIELD PROBING
0.,15.
 INPUT THE DISTANCE BETWEEN FIELD POINT IN FEET
0.1
 DO YOU WANT GO TERM?  IF YES, TYPE 1
1
 DO YOU WANT JUNCTION DIFFRACTION?  IF YES TYPE 1
1
 DO YOU WANT SKIRT DIFFRACTION?  IF YES, TYPE 1
1
 DO YOU WANT FEED BLOCKAGE?  IF YES, TYPE 1
0
 DO YOU WANT ELECTRIC FIELD COMPONENTS?  IF YES, TYPE 1
0
 INPUT THE DISTANCE OF THE JUNCTION FROM THE CENTER
 OF THE PARABOLOID IN FEET
15.
```

In Figure 11, the amplitude of the scattered magnetic field is plotted versus the vertical displacement. Note that the scattered field magnitude decreases with an increase in the vertical displacement. The drop in the scattered field is due to the drop in the specularly reflected field which is shown in Figure 12. In this cut, the feed has uniform pattern. However, the distance between the point of reflection and the feed increases with an increase in the vertical displacement. The decrease in the incident field results in a drop in the reflected field. The total scattered field oscillates around the specularly reflected field. These oscillations are due to the junction and skirt diffractions. The ripple size of the oscillations for vertical displacements between 3.5 feet and 13.5 feet is less than 0.2 dB. Thus, the diffracted fields in this region are quite small which is further verified by the results shown in Figures 13 and 14, where the junction

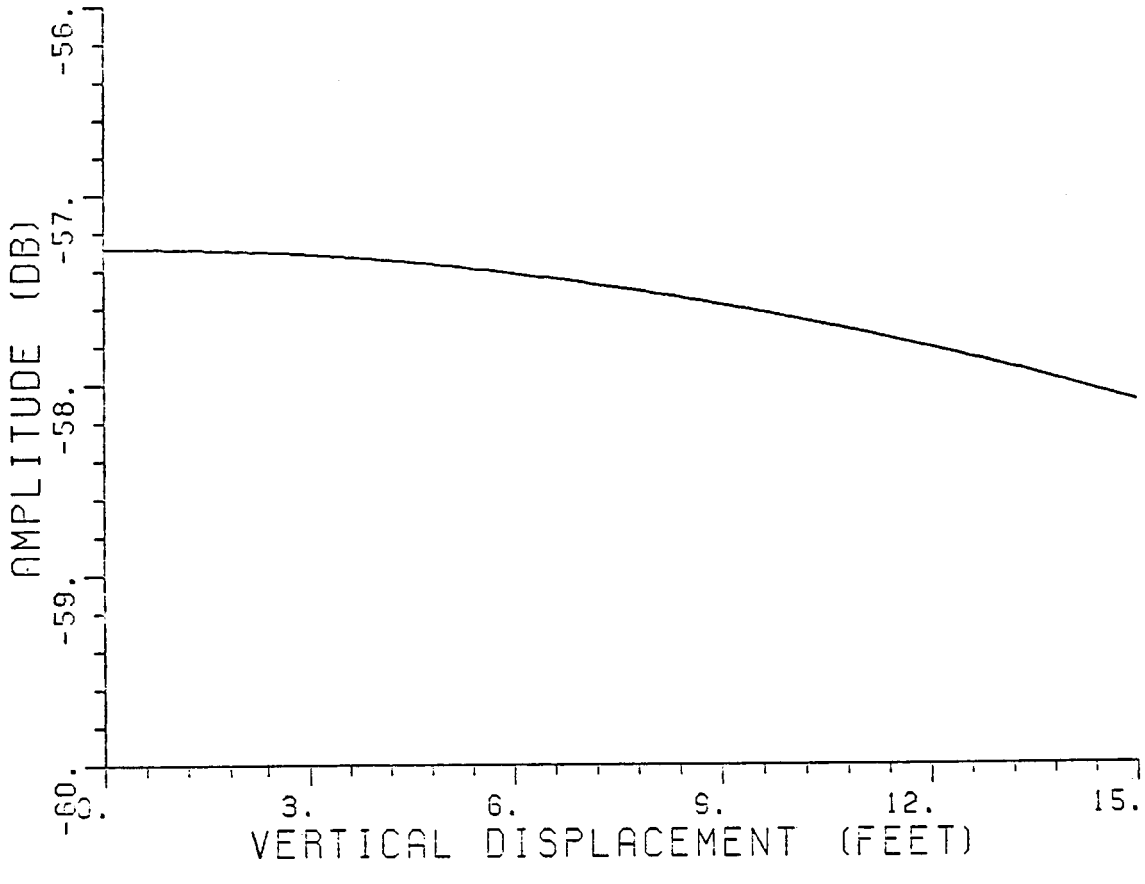

Figure 12. The specularly reflected field component versus vertical displacement. Note that ϕ=0°, and feed is a short horizontal magnetic dipole.

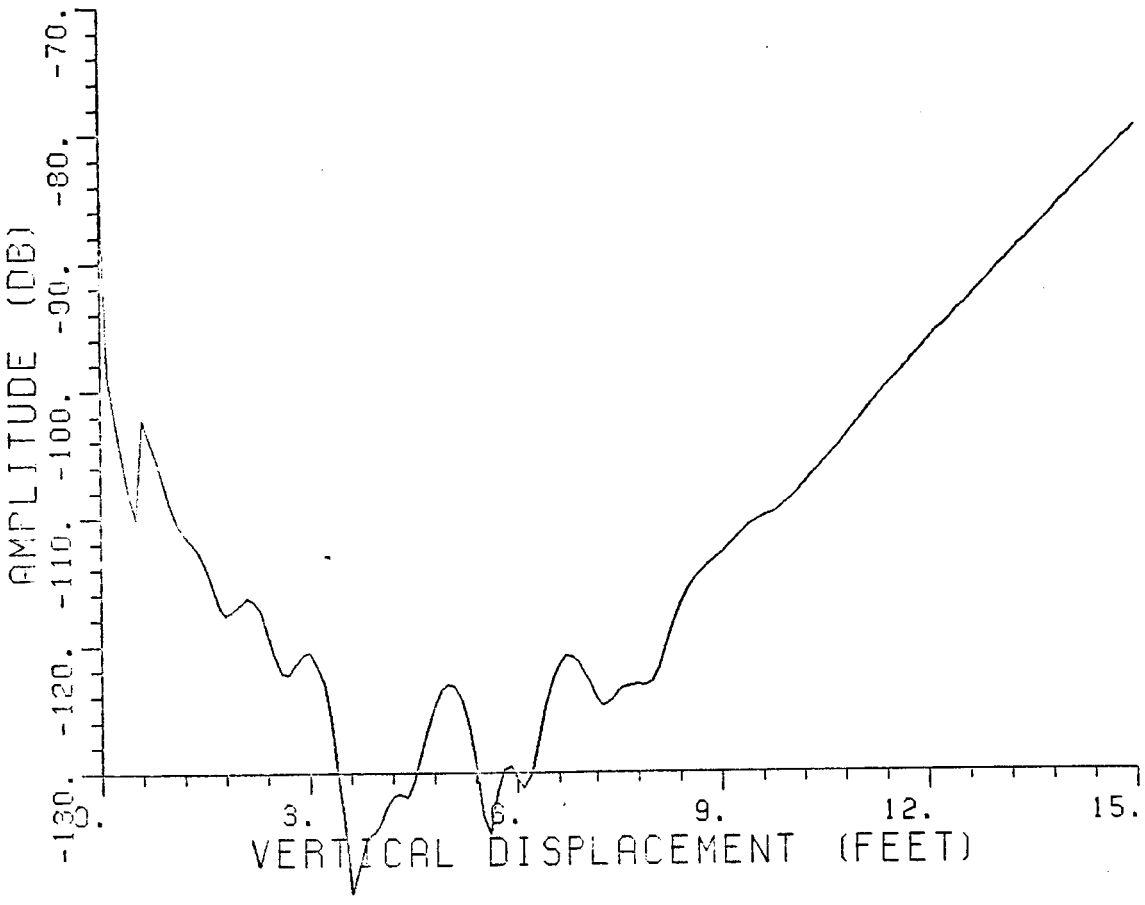

Figure 13. The junction diffracted field component versus vertical displacement. Note that ϕ=0° and the feed is a short horizontal magnetic dipole.

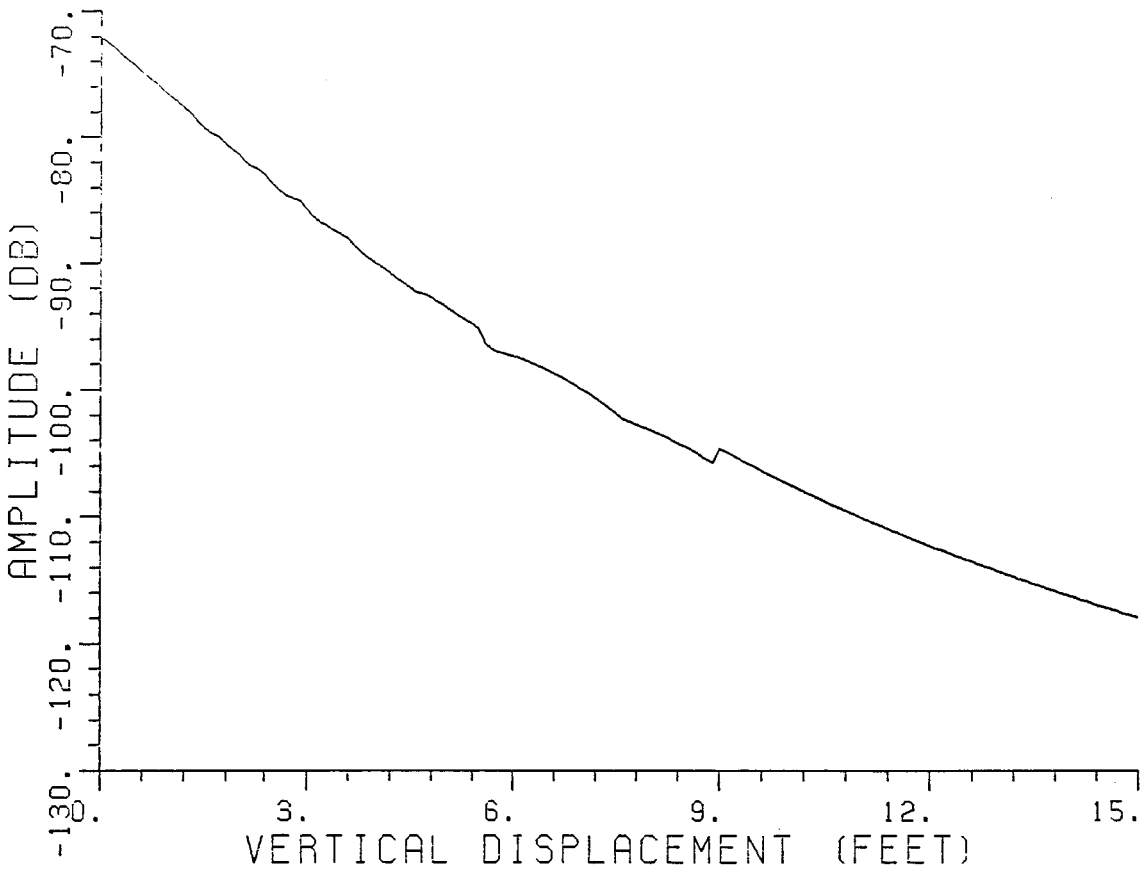

Figure 14. The skirt diffracted field component versus vertical displacement. Note that $\phi=0°$, and the feed is a short horizontal magnetic dipole.

diffraction and the skirt diffraction are plotted, respectively, versus the vertical displacement. Note that each term is plotted relative to the same level so that results can be compared. As expected the skirt diffraction is dominant for small vertical displacements; whereas, the junction diffraction is dominant near the edge of the paraboloid (vertical displacement equal to 15 feet). Thus for vertical displacements between 3.5 feet and 13.5 feet, the major variation in the scattered field is due to the specular reflection. To decrease this variation or taper in the field, one should change the illumination of the reflector.

Figure 15 shows the x component of the scattered magnetic field when the short magnetic dipole used as the feed in the previous example is oriented along the x_f axis (see Figure 6). All other parameters are the same as before. The input data set is as follows:

```
 INPUT THE FREQUENCY IN GHz.
2.
 INPUT THE DISTANCE OF THE FOCAL POINT FROM THE
 CENTER OF THE PARABOLOID IN FEET
24.
 INPUT THE TILT ANGLE OF THE FEED
0.
 INPUT THE MAGNITUDE OF THE MAGNETIC DIPOLES
 ALONG X AND Y AXES
1.,0.
 INPUT THE MAGNITUDE OF THE ELECTRIC DIPOLES
 ALONG X AND Y AXES
0.,0.
 INPUT THE DISTANCE OF THE FIELD PLANE FROM THE CENTER
 OF THE PARABOLOID IN FEET
36.
 INPUT THE PHI CUT IN DEGREES
0.
  INPUT START POINT AND END POINT FOR FIELD PROBING
0.,15.
 INPUT THE DISTANCE BETWEEN FIELD POINTS IN FEET
0.1
 DO YOU WANT GO TERM?  IF YES, TYPE 1
1
```

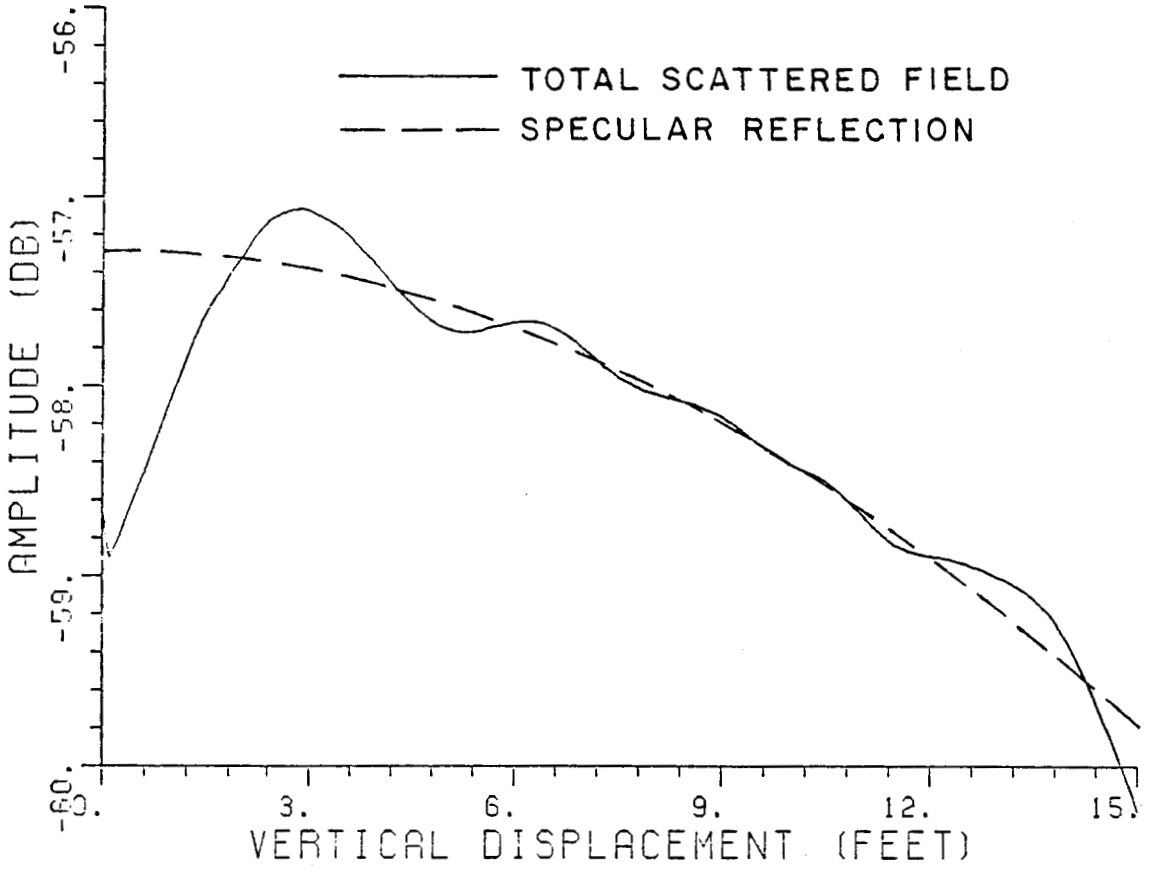

Figure 15. Co-polarized (x) component of the scattered magnetic versus vertical displacement. Note that ϕ=0°, and the feed is a short vertical magnetic dipole. Various mechanisms included in the scattered field are:

1. Specular reflection
2. Junction diffraction
3. Skirt diffraction

```
 DO YOU WANT JUNCTION DIFFRACTION?  IF YES TYPE 1
1
 DO YOU WANT SKIRT DIFFRACTION?  IF YES, TYPE 1
1
 DO YOU WANT FEED BLOCKAGE?  IF YES, TYPE 1
0
 DO YOU WANT ELECTRIC FIELD COMPONENTS?  IF YES, TYPE 1
0
 INPUT THE DISTANCE OF THE JUNCTION FROM THE CENTER
 OF THE PARABOLOID IN FEET
15.
```

For this feed also the cross-polarized (y) component in the vertical cut is negligible. Again the scattered field drops with an increase in the vertical displacement. The drop in the scattered field is again due to the drop in the specularly reflected field. The specularly reflected field is shown by the broken curve in Figure 15. Comparing the results shown in Figures 11 and 15, one can see that for the vertical oriented magnetic dipole (along x_f), the drop in the scattered field is more than that for the horizontally oriented magnetic dipole. The reason for this behavior is that the vertical dipole does not have a uniform radiation pattern in a vertical cut. Instead the radiation intensity is the maximum for $\theta=0°$ (or a zero vertical displacement) and it decreases with an increase in θ. Thus, the drop in the reflected field versus vertical displacement is larger in this case. Again the variation in the scattered field due to the junction and skirt diffractions for vertical displacement between 3.5 and 13.5 feet are quite small.

In the case of the vertical magnetic dipole, one can tilt the dipole such that its radiation intensity is a maximum near the edge of the paraboloid. In this case, the drop in the incident field near the reflector edge due to the increase in the distance from the feed will be

compensated by the increase in the radiation intensity. Thus, the specularly reflected will be more uniform in a vertical cut. However, the specularly reflected field in other cuts ($\phi \neq 0°$) will not be uniform. Other feed configurations, therefore, should be tested.

Figures 16 and 17 show the scattered magnetic field in the vertical cut when the feed is a short electric dipole oriented along x_f and y_f, respectively. All other parameters are the same as before. The input data for these two examples are given below.

i) **Input data for vertical electric dipole:**

```
 INPUT THE FREQUENCY IN GHz.
2.
 INPUT THE DISTANCE OF THE FOCAL POINT FROM THE
 CENTER OF THE PARABOLOID IN FEET
24.
 INPUT THE TILT ANGLE OF THE FEED
0.
 INPUT THE MAGNITUDE OF THE MAGNETIC DIPOLES
 ALONG X AND Y AXES
0.,0.
 INPUT THE MAGNITUDE OF THE ELECTRIC DIPOLES
 ALONG X AND Y AXES
1.,0.
 INPUT THE DISTANCE OF THE FIELD PLANE FROM THE CENTER
 OF THE PARABOLOID IN FEET
36.
 INPUT THE PHI CUT IN DEGREES
0.
 INPUT START POINT AND END POINT FOR FIELD PROBING
0.,15.
 INPUT THE DISTANCE BETWEEN FIELD POINTS IN FEET
0.1
 DO YOU WANT GO TERM?  IF YES, TYPE 1
1
 DO YOU WANT JUNCTION DIFFRACTION?  IF YES TYPE 1
1
 DO YOU WANT SKIRT DIFFRACTION?  IF YES, TYPE 1
1
 DO YOU WANT FEED BLOCKAGE?  IF YES, TYPE 1
0
```

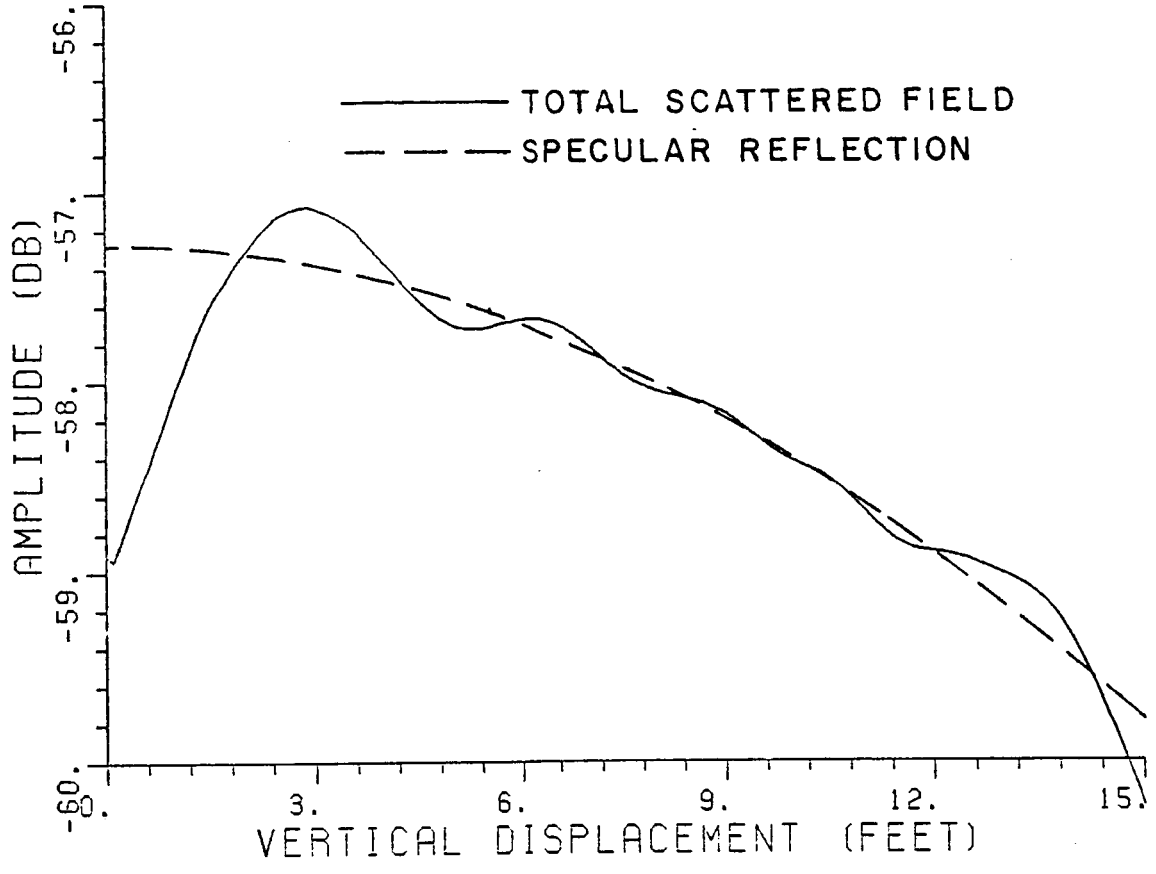

Figure 16. Co-polarized (y) component of the scattered magnetic field versus vertical displacement. Note that $\phi=0°$, and the feed is a short vertical electrical dipole. Various mechanisms included in the scattered field are:

1. Specular reflection
2. Junction diffraction
3. Skirt diffraction

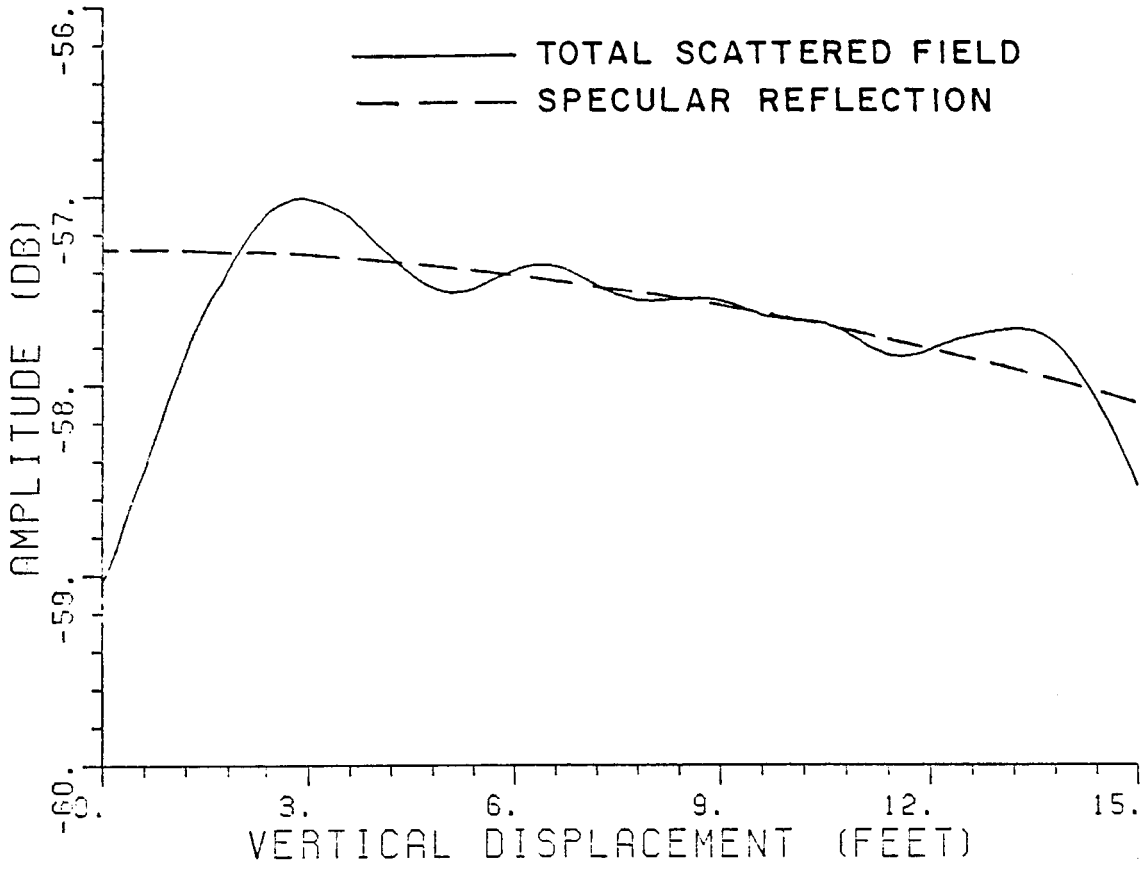

Figure 17. Co-polarized (x) component of the scattered magnetic field versus vertical displacement. Note that ϕ=0°, and the feed is a short horizontal electric dipole. Various mechanism included in the scattered field are:

1. Specular reflection
2. Junction diffraction
3. Skirt diffraction

```
 DO YOU WANT ELECTRIC FIELD COMPONENTS?  IF YES, TYPE 1
0
 INPUT THE DISTANCE OF THE JUNCTION FROM THE CENTER
 OF THE PARABOLOID IN FEET
15.
```

ii) **Input data for horizontal electric dipole:**

```
 INPUT THE FREQUENCY IN GHz.
2.
 INPUT THE DISTANCE OF THE FOCAL POINT FROM THE
 CENTER OF THE PARABOLOID IN FEET
24.
 INPUT THE TILT ANGLE OF THE FEED
0.
 INPUT THE MAGNITUDE OF THE MAGNETIC DIPOLES
 ALONG X AND Y AXES
0.,0.
 INPUT THE MAGNITUDE OF THE ELECTRIC DIPOLES
 ALONG X AND Y AXES
0.,1.
 INPUT THE DISTANCE OF THE FIELD PLANE FROM THE CENTER
 OF THE PARABOLOID IN FEET
36.
 INPUT THE PHI CUT IN DEGREES
0.
 INPUT START POINT AND END PIONT FOR FIELD PROBING
0.,15.
 INPUT THE DISTANCE BETWEEN FIELD POINTS IN FEET
0.1
 DO YOU WANT GO TERM?  IF YES, TYPE 1
1
 DO YOU WANT JUNCTION DIFFRACTION?  IF YES, TYPE 1
1
 DO YOU WANT SKIRT DIFFRACTION?  IF YES, TYPE 1
1
 DO YOU WANT FEED BLOCKAGE?  IF YES, TYPE 1
0
 DO YOU WANT ELECTRIC FIELD COMPONENTS?  IF YES, TYPE 1
0
 INPUT THE DISTANCE OF THE JUNCTION FROM THE CENTER
 OF THE PARABOLOID IN FEET
15.
```

The specularly reflected fields for the two feeds are also shown in Figures 16 and 17. The cross polarized scattered field for these two feeds in the vertical cut is again negligible. From the plots in Figures 16 and 17, one can draw the same conclusions as before.

In all examples considered above, the major variation in the scattered field was due to non-uniform illumination of the reflector. One way to get a more uniform reflector illumination is to use a Huygen source as the feed and tilt the feed such that the radiation intensity of the feed is maximum near the top edge of the paraboloid. Figure 18 shows the scattered field of the reflector in the vertical cut when the feed is a Huygen source (one short electric dipole oriented along x_f and another short magnetic dipole oriented along y_f). The feed is tilted by 17.45°. The input data set for this case is as follows:

```
 INPUT THE FREQUENCY IN GHz.
2.
 INPUT THE DISTANCE OF THE FOCAL POINT FROM THE
 CENTER OF THE PARABOLOID IN FEET
24.
 INPUT THE TILT ANGLE OF THE FEED
17.45
 INPUT THE MAGNITUDE OF THE MAGNETIC DIPOLES
 ALONG X AND Y AXES
0.,1.
 INPUT THE MAGNITUDE OF THE ELECTRIC DIPOLES
 ALONG X AND Y AXES
1.,0.
 INPUT THE DISTANCE OF THE FIELD PLANE FROM THE CENTER
 OF THE PARABOLOID IN FEET
36.
 INPUT THE PHI CUT IN DEGREES
0.
 INPUT START POINT AND END POINT FOR FIELD PROBING
0.,15.
 INPUT THE DISTANCE BETWEEN FIELD POINTS IN FEET
0.1
 DO YOU WANT GO TERM?  IF YES, TYPE 1
1
 DO YOU WANT JUNCTION DIFFRACTION?  IF YES TYPE 1
1
 DO YOU WANT SKIRT DIFFRACTION?  IF YES, TYPE 1
1
 DO YOU WANT FEED BLOCKAGE?  IF YES, TYPE 1
0
```

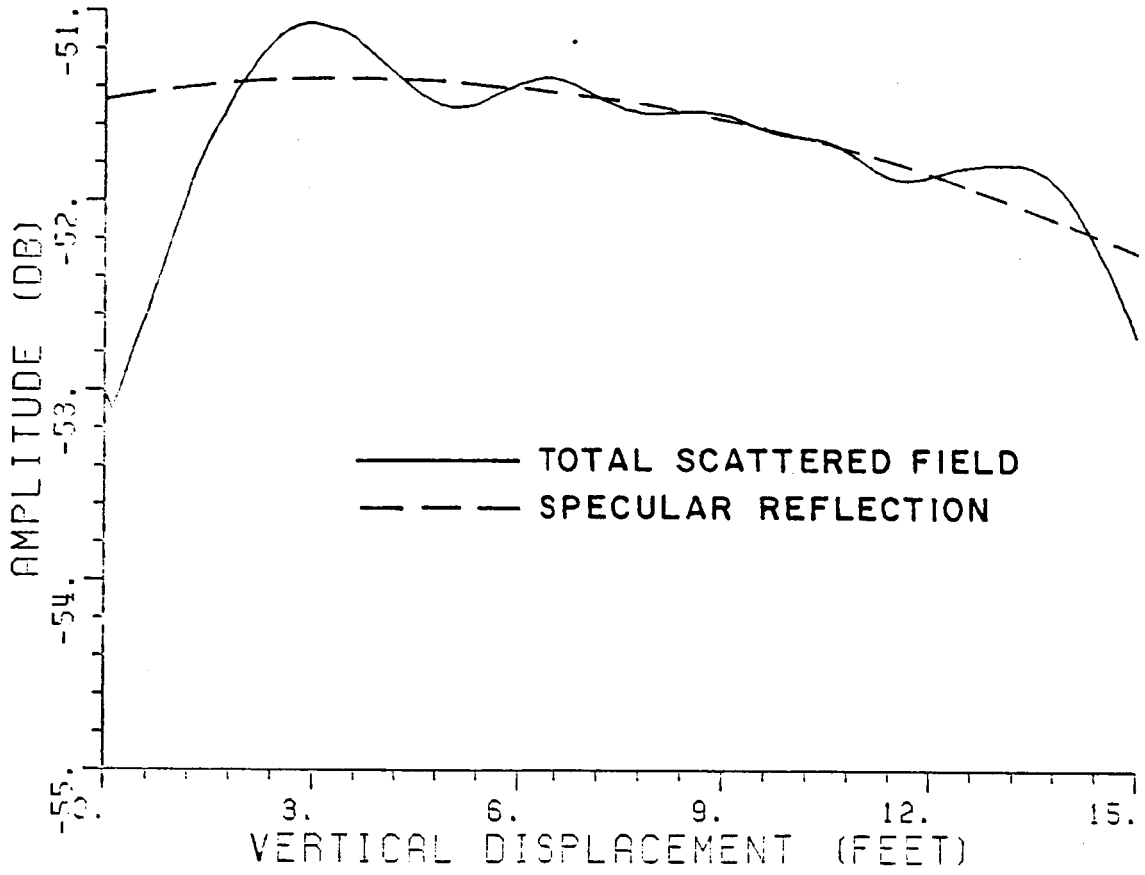

Figure 18. Co-polarized (y) component of the scattered magnetic field versus vertical displacement. Note that ϕ=0°, and the feed is a Huygen's source tilted by 17.45°. Various mechanisms included in the field computation are:

1. Specular reflection
2. Junction diffraction
3. Skirt diffraction

```
 DO YOU WANT ELECTRIC FIELD COMPONENTS?  IF YES, TYPE 1
0
 INPUT THE DISTANCE OF THE JUNCTION FROM THE CENTER
 OF THE PARABOLOID IN FEET
15.
```

In Figure 18, the co-polarized (y) component of the scattered magnetic field is plotted versus the vertical displacement. Again the cross-polarized component of the scattered field is very small and, therefore, is not shown. The various scattering mechanisms included in the field computation are: the specular reflection, the junction diffraction and the skirt diffraction. The specularly reflected field is shown by the broken curve in the figure. Comparing the specular reflection in this case with previous examples (see Figures 12, 15, 16 and 17), one can see that the drop in the specularly reflected field for a vertical displacement between 3 feet and 12 feet is the smallest for the Huygen's source. However, even for the Huygen's source, the scattered field drops by approximatley 0.5 dB. Therefore, the tilt angle of the feed should be increased. Again the ripple size of the oscillations in the scattered field for vertical displacements between 3.5 feet and 13.5 feet is less than 0.2 dB.

Figure 19 shows the scattered field when the tilt angle of the feed is increased to 30°. All other parameters are the same as before. The specularly reflected component of the scattered field is shown by the broken curve in the figure. One can see that the specularly reflected field does not vary much with vertical displacement. For vertical displacements between 0 and 12 feet, the variation in the specular reflection is less than 0.3 dB. Thus, this feed is desirable if a more

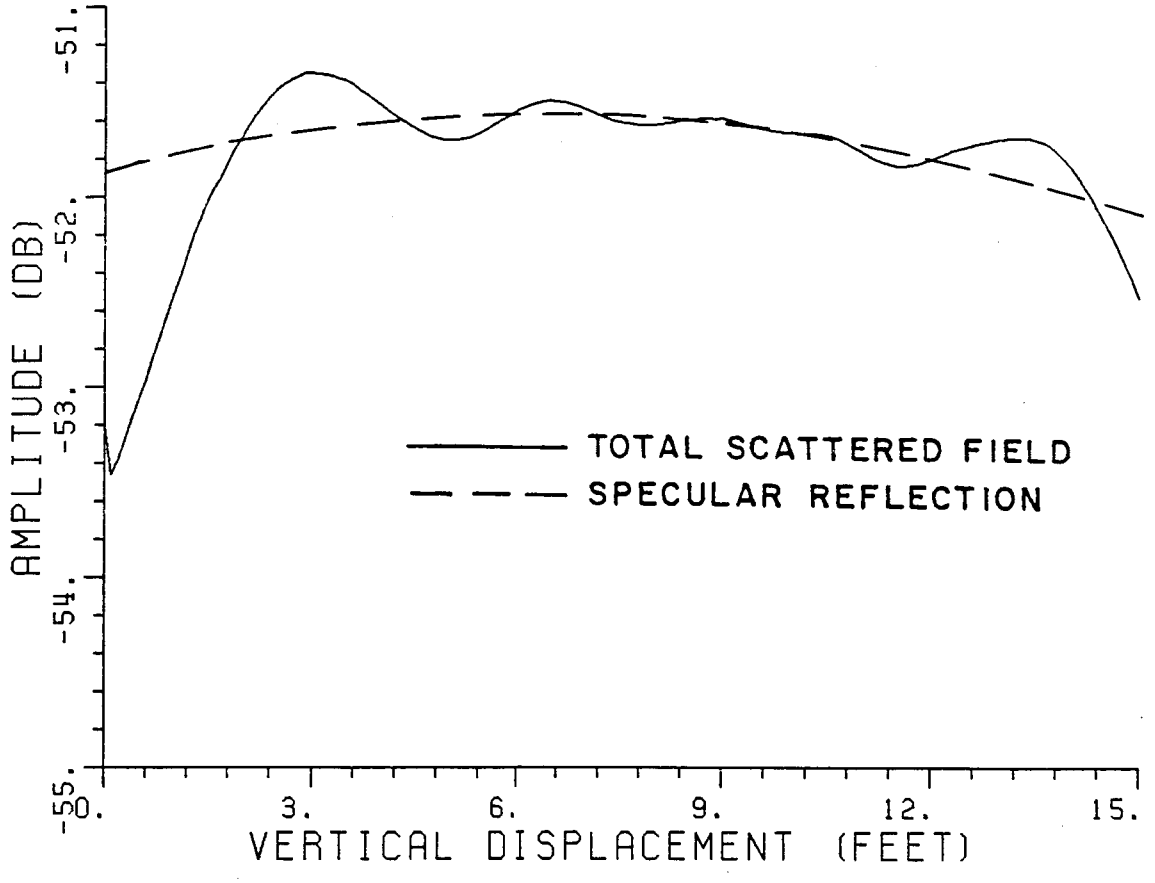

Figure 19. Co-polarized (y) component of the scattered magnetic field versus vertical displacement. Note that ϕ=0°, and the feed is a Huygen's source tilted by 30°. Various mechanisms included in the field computation are:

1. Specular reflection
2. Junction diffraction
3. Skirt diffraction

uniform aperture illumination is required. The input data set for this example is given below:

```
 INPUT THE FREQUENCY IN GHz.
2.
 INPUT THE DISTANCE OF THE FOCAL POINT FROM THE
 CENTER OF THE PARABOLOID IN FEET
24.
 INPUT THE TILT ANGLE OF THE FEED
30.
 INPUT THE MAGNITUDE OF THE MAGNETIC DIPOLES
 ALONG X AND Y AXES
0.,1.
 INPUT THE MAGNITUDE OF THE ELECTRIC DIPOLES
 ALONG X AND Y AXES
1.,0.
 INPUT THE DISTANCE OF THE FIELD PLANE FROM THE CENTER
 OF THE PARABOLOID IN FEET
36.
 INPUT THE PHI CUT IN DEGREES
0.
 INPUT START POINT AND END POINT FOR FIELD PROBING
0.,15.
 INPUT THE DISTANCE BETWEEN FIELD POINTS IN FEET
0.1
 DO YOU WANT GO TERM?  IF YES, TYPE 1
1
 DO YOU WANT JUNCTION DIFFRACTION?  IF YES TYPE 1
1
 DO YOU WANT SKIRT DIFFRACTION?  IF YES, TYPE 1
1
 DO YOU WANT FEED BLOCKAGE?  IF YES, TYPE 1
0
 DO YOU WANT ELECTRIC FIELD COMPONENTS?  IF YES, TYPE 1
0
 INPUT THE DISTANCE OF THE JUNCTION FROM THE CENTER
 OF THE PARABOLOID IN FEET
15.
```

The total scattered field in Figure 19 oscillates around the specularly reflected field. As pointed out before, these oscillations are due to the junction and skirt diffractions. Again the ripple size of the oscillations for vertical displacements between 3.5 and 13.5 feet is within 0.2 dB. Thus, the junction and skirt diffractions are quite

small as can be seen from the results shown in Figures 20 and 21, where the junction and skirt diffracted fields are, respectively, plotted versus the vertical displacement. These plots were obtained from the output data stored on units #21 and 22, respectively. Again, as expected, the junction diffraction is strong near the edge of the paraboloid (vertical displacement ~ 15 feet) while the skirt diffraction is strong near the bottom of the reflector. The slope of the junction diffracted field is more than that of the skirt diffracted field. Thus, the usable target zone lost due the skirt diffraction will be more than that due to the junction diffraction. This is clear from the total scattered field plot in Figure 19. Assuming that the maximum tolerable ripple is 0.2 dB, one loses approximately 3.5 feet in terms of target zone dimensions due to the skirt diffraction while only 1.5 feet is lost due to the junction diffraction. The reason for this is that the junction between the skirt and the paraboloid is smooth only to first order (only slope is continuous) while the junction between the paraboloid and the blended rolled edge is smooth to third order (first three derivatives are continuous).

In the above discussion, the feed blockage was not included in the scattered field computation. The feed blockage also affects the fields in the target zone. Therefore, to complete the discussion, the feed blockage is computed next.

Figure 22 shows the y component of the scattered magnetic field due to the feed blockage in the vertical cut versus the vertical displacement. The feed aperture is assumed to be a 12" x 12" (2λ x 2λ) flat rectangular plate. The input data set for this example is given below:

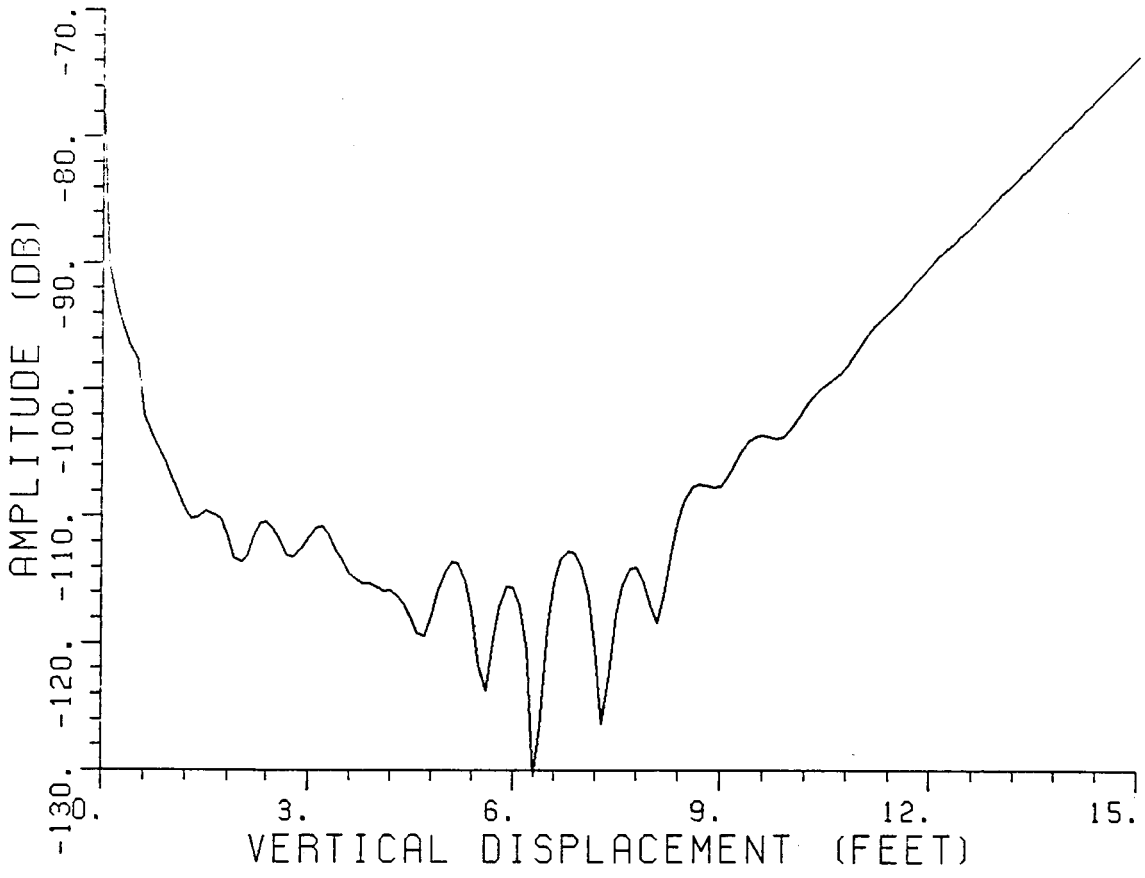

Figure 20. Junction diffracted field component versus vertical displacement. Note that $\phi=0°$, and the feed is a Huygen's source tilted by 30°.

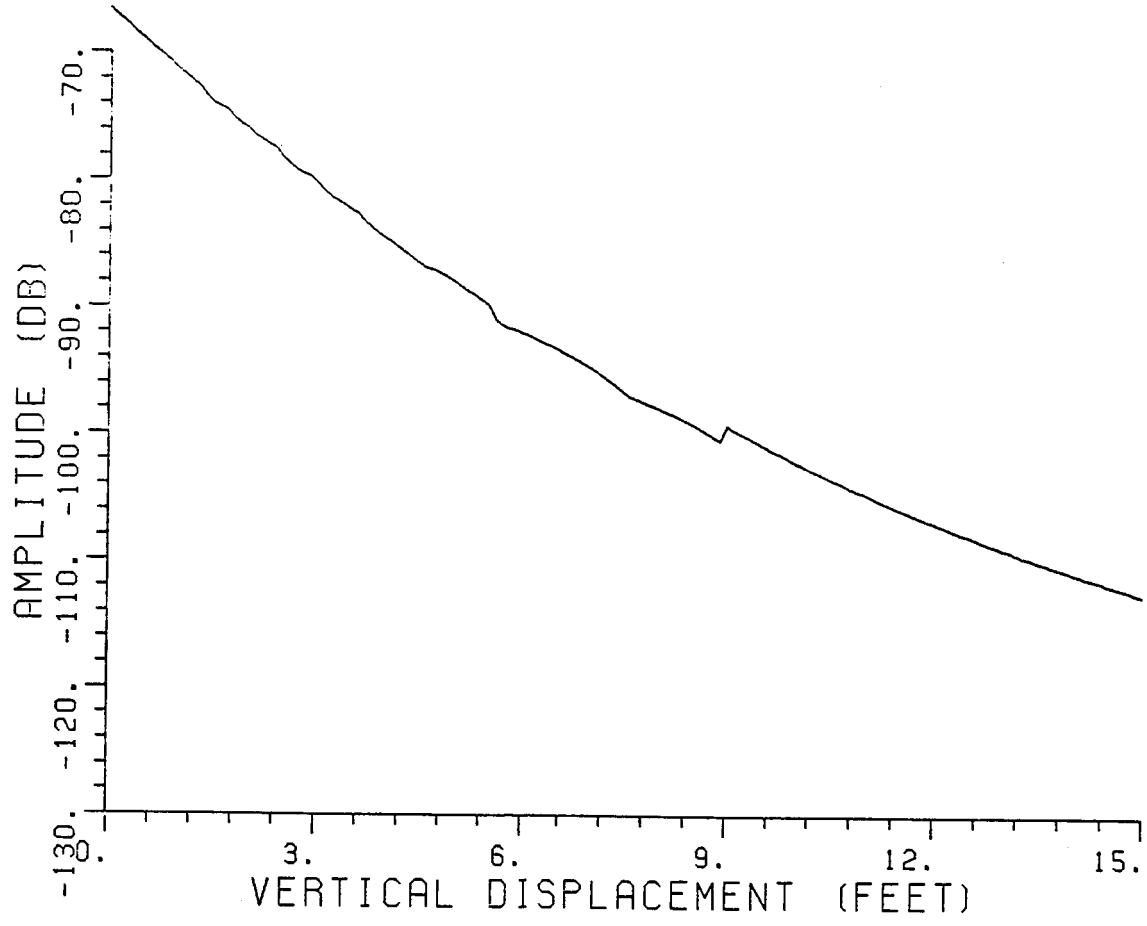

Figure 21. Skirt diffracted field component versus vertical displacement. Note that ϕ=0°, and the feed is a Huygen's source tilted by 30°.

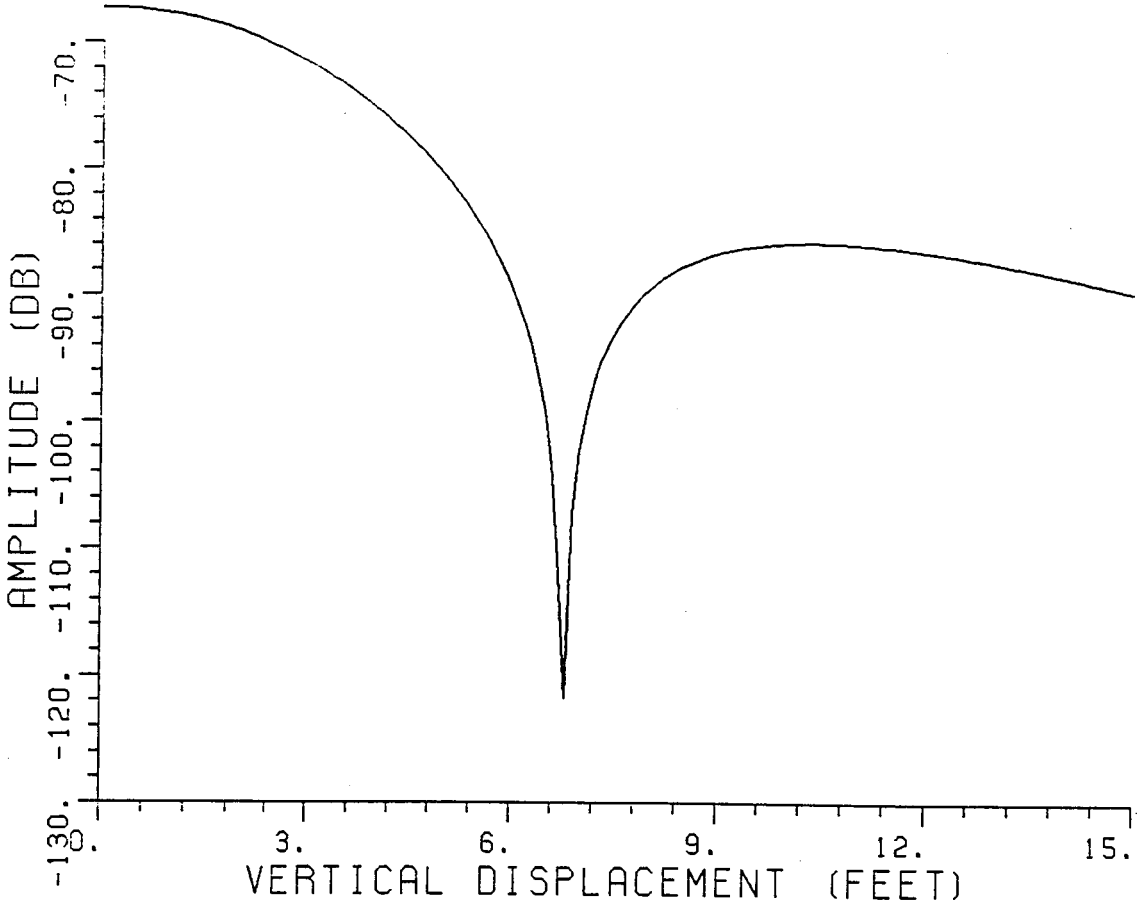

Figure 22. Co-polarized (y) component of the feed blockage versus vertical displacement. Note that ϕ=0°, the feed is a Huygen's source tilted by 30°, and feed aperture is 12" x 12".

```
 INPUT THE FREQUENCY IN GHz.
2.
 INPUT THE DISTANCE OF THE FOCAL POINT FROM THE
 CENTER OF THE PARABOLOID IN FEET
24.
 INPUT THE TILT ANGLE OF THE FEED
30.
 INPUT THE MAGNITUDE OF THE MAGNETIC DIPOLES
 ALONG X AND Y AXES
0.,1.
 INPUT THE MAGNITUDE OF THE ELECTRIC DIPOLES
 ALONG X AND Y AXES
1.,0.
 INPUT THE DISTANCE OF THE FIELD PLANE FROM THE CENTER
 OF THE PARABOLOID IN FEET
36.
 INPUT THE PHI CUT IN DEGREES
0.
 INPUT START POINT AND END POINT FOR FIELD PROBING
0.,15.
 INPUT THE DISTANCE BETWEEN FIELD POINTS IN FEET
0.1
 DO YOU WANT GO TERM?  IF YES, TYPE 1
0
 DO YOU WANT JUNCTION DIFFRACTION?  IF YES TYPE 1
0
 DO YOU WANT SKIRT DIFFRACTION?  IF YES, TYPE 1
0
 DO YOU WANT FEED BLOCKAGE?  IF YES, TYPE 1
1
 DO YOU WANT ELECTRIC FIELD COMPONENTS?  IF YES, TYPE 1
0
 INPUT THE Z LOCATION OF THE FEED APERTURE IN FEET
24.
 INPUT THE NUMBER OF CORNERS IN FEED APERTURE
4.
 INPUT THE X,Y COORDINATES OF THE CORNERS IN INCHES
6.,6.,-6.,6.,-6.,-6.,6.,-6.
```

Note that all other parameters are the same as before. The cross-polarized (x) component of the scattered field is very small and is therefore not shown here. Comparing the feed blockage with the specularly reflected field (see Figure 19), one can see that the feed blockage is quite large (within 15 dB of the specularly reflected

field). Thus, the feed blockage will cause large oscillations in the fields in the target zone as shown in Figure 23. In Figure 23, the vector sum of the specular reflected field and the feed blockage is plotted versus the vertical displacement. The specularly reflected field is shown by the broken curve in the figure. Note that the amplitude of the oscillations, especially for small vertical displacements, is quite large. Even for large vertical displacements (~ 15 feet), the ripple size is more than 0.2 dB. Thus, the feed blockage is quite a serious problem. To increase the size of the sweet spot, the feed blockage must be reduced.

One way to decrease the feed blockage is to decrease the size of the feed. Figure 24 shows the scattered field magnitude due to the feed blockage when the size of the feed aperture is reduced to 6" x 6" (λ x λ). All other parameters are the same as before. Note that the feed blockage, especially for small vertical displacements, has decreased significantly. Thus, the ripple size of the oscillation in the scattered field should decrease as verified by the results shown in Figure 25. In Figure 25, the total scattered field due to the specular reflection and the feed blockage is plotted versus the vertical displacement. Comparing the results shown in Figures 23 and 25, one can see that the ripple size has decreased. However, even for a 6" x 6" feed aperture (Figure 25) for vertical displacements less than 7 feet, the ripple is more than 0.2 dB. Thus, the size of the feed should be reduced further.

Figure 26 shows the feed blockage when the size of the feed aperture is reduced to 3" x 3" $(\frac{\lambda}{2} \times \frac{\lambda}{2})$. All other parameters are the

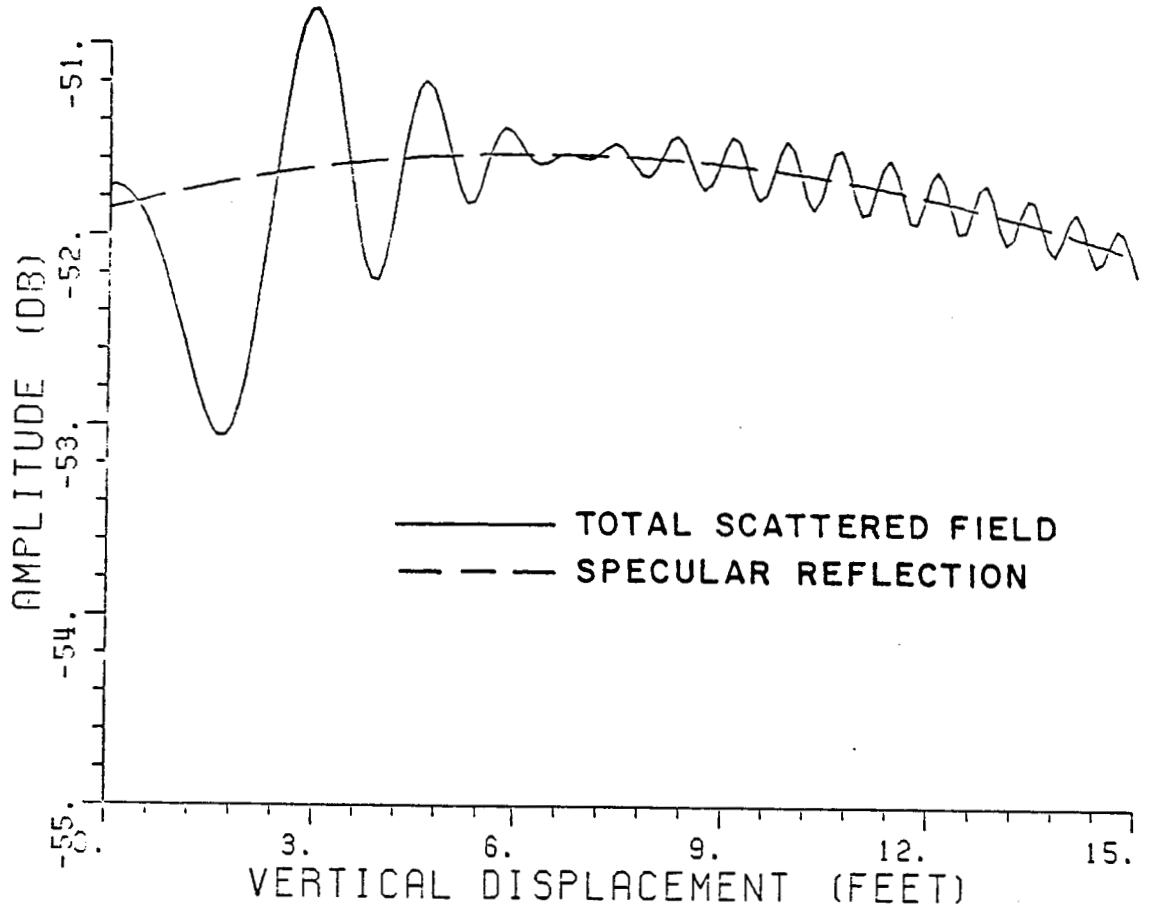

Figure 23. Co-polarized (y) component of the scattered magnetic field versus vertical displacement. Note that ϕ=0°, the feed is a Huygen's source tilted by 30°, the feed aperture is 12" x 12", and various mechanisms included in the scattered field are:

1. Specular reflection
2. Feed blockage

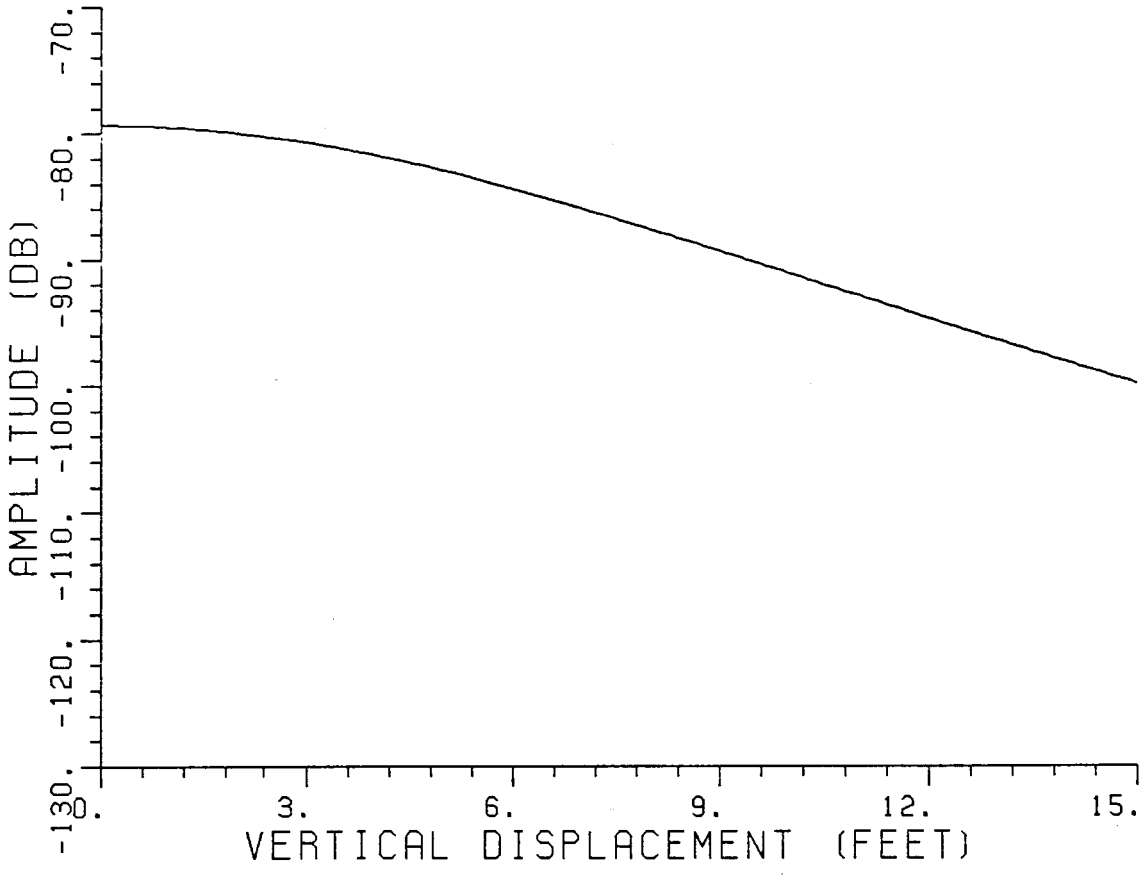

Figure 24. Co-polarized (y) component of the feed blockage versus vertical displacement. Note that $\phi=0°$, the feed is a Huygen's source tilted by 30° and the feed aperture is 6" x 6".

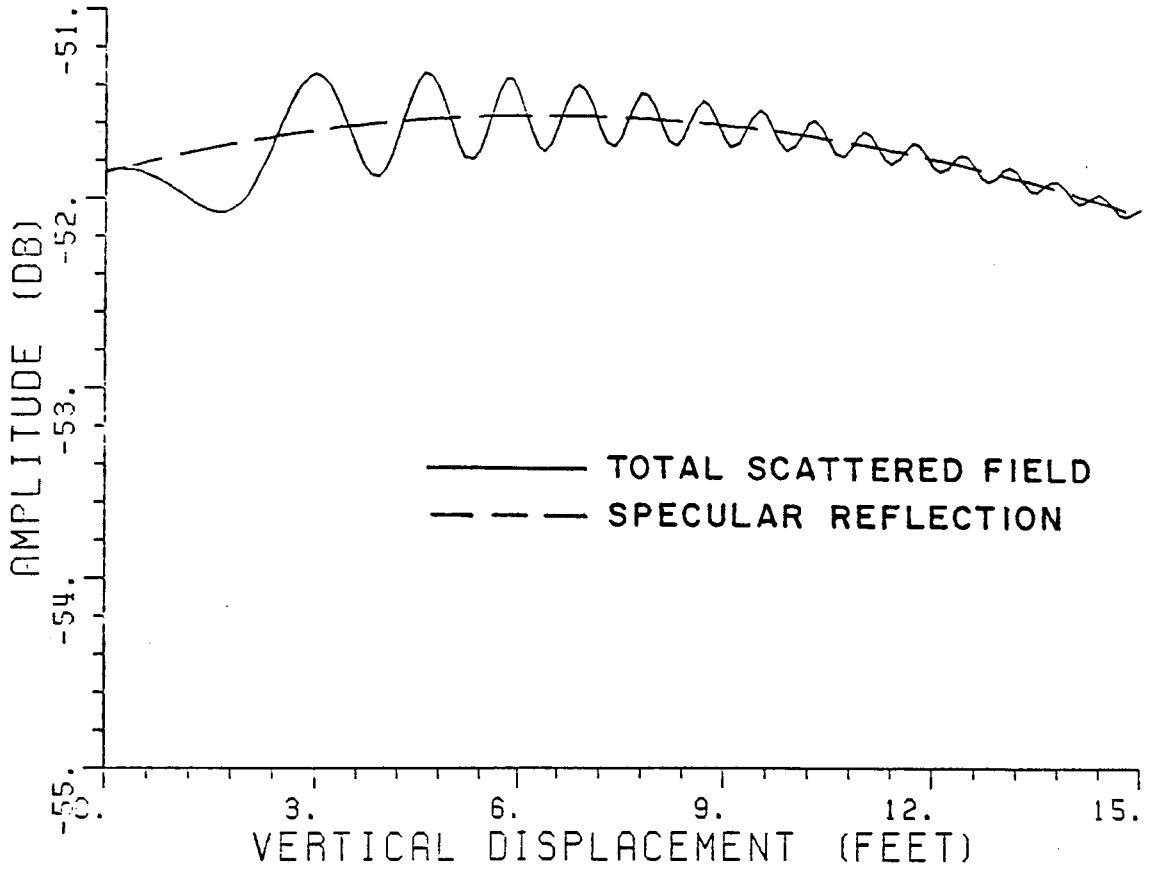

Figure 25. Co-polarized (y) component of the scattered magnetic field versus vertical displacement. Note that ϕ=0°, the feed is a Huygen's source tilted by 30°, the feed aperture is 6" x 6", and various mechanisms included in the scattered field are:

1. Specular reflection
2. Feed blockage

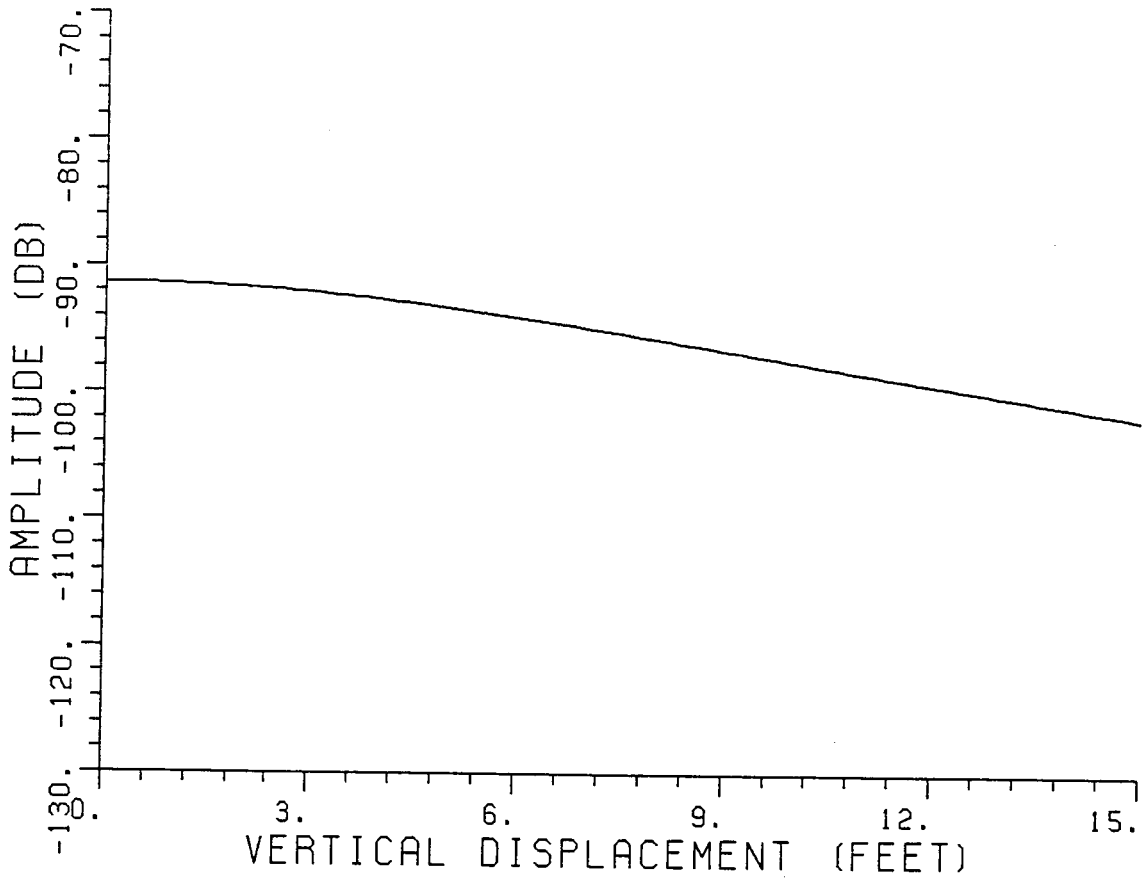

Figure 26. Co-polarized (y) component of the feed blockage versus vertical displacement. Note that ϕ=0°, the feed is a Huygen's source tilted by 30°, and the feed aperture is 3" x 3".

same as before. Comparing the plots in Figures 22, 24 and 26, one can see that the feed blockage, especially for small vertical displacements, has reduced by more than 20 dB. Thus, the ripple size of the oscillations due to the feed blockage should reduce as can be seen in the plots of Figure 27. In Figure 27, the vector sum of the specularly reflected field and the feed blockage is plotted versus the vertical displacement. The specularly reflected field alone is also plotted in the figure. Note that the ripple size of the oscillations in Figure 27 is quite small (less than 0.2 dB). This feed is used in the rest of the study.

Figure 28 shows the total scattered field in the xz plane (ϕ=0°cut) when all four mechanisms are included in the field computation. The feed is a Huygen source tilted by 30°. The feed aperture is a 3" x 3" flat rectangular plate. The input data set is as follows.

```
 INPUT THE FREQUENCY IN GHz.
2.
 INPUT THE DISTANCE OF THE FOCAL POINT FROM THE
 CENTER OF THE PARABOLOID IN FEET
24.
 INPUT THE TILT ANGLE OF THE FEED
30.
 INPUT THE MAGNITUDE OF THE MAGNETIC DIPOLES
 ALONG X AND Y AXES
0.,1.
 INPUT THE MAGNITUDE OF THE ELECTRIC DIPOLES
 ALONG X AND Y AXES
1.,0.
 INPUT THE DISTANCE OF THE FIELD PLANE FROM THE CENTER
 OF THE PARABOLOID IN FEET
36.
 INPUT THE PHI CUT IN DEGREES
0.
 INPUT START POINT AND END POINT FOR FIELD PROBING
0.,15.
 INPUT THE DISTANCE BETWEEN FIELD POINTS IN FEET
0.1
```

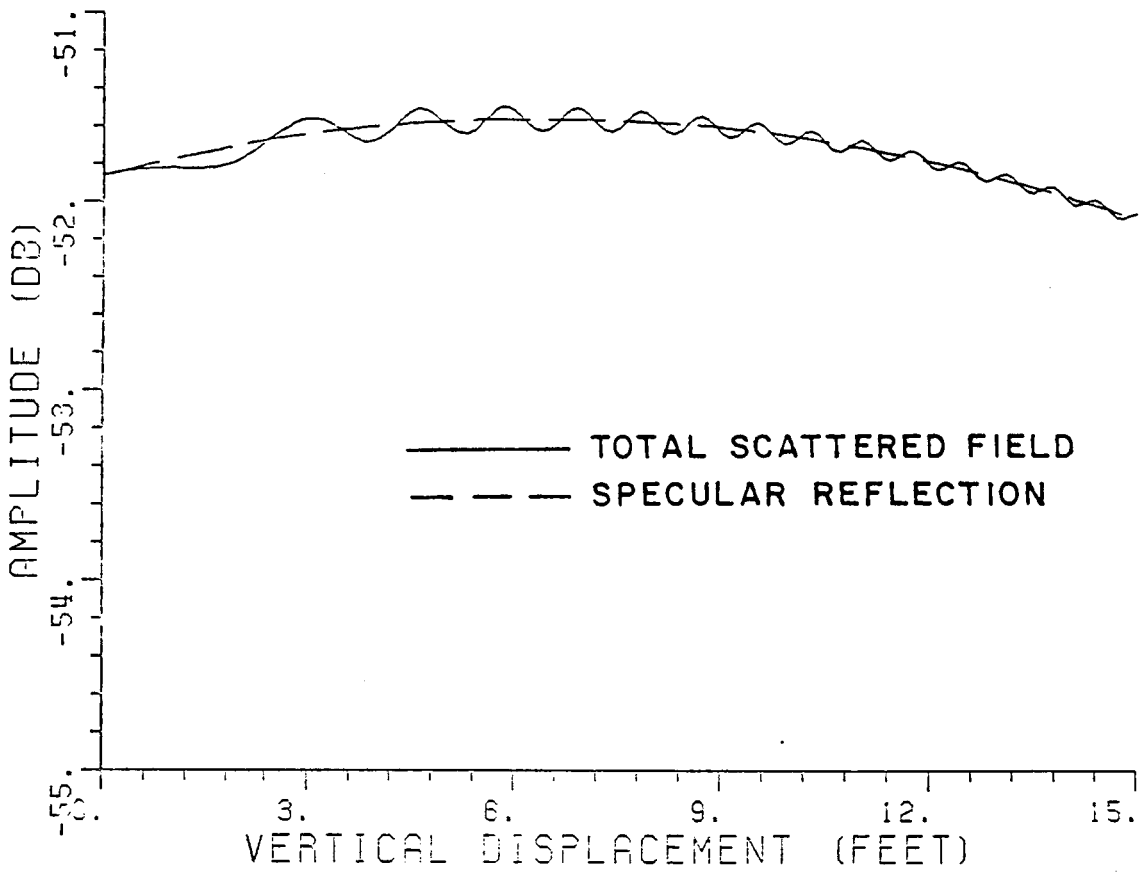

Figure 27. Co-polarized (y) component of the scattered magnetic field versus vertical displacement. Note that ϕ=0°, the feed is a Huygen's source tilted by 30°, and the feed aperture is 3" x 3". Various mechanisms included in the scattered field are:

1. Specular reflection
2. Feed blockage

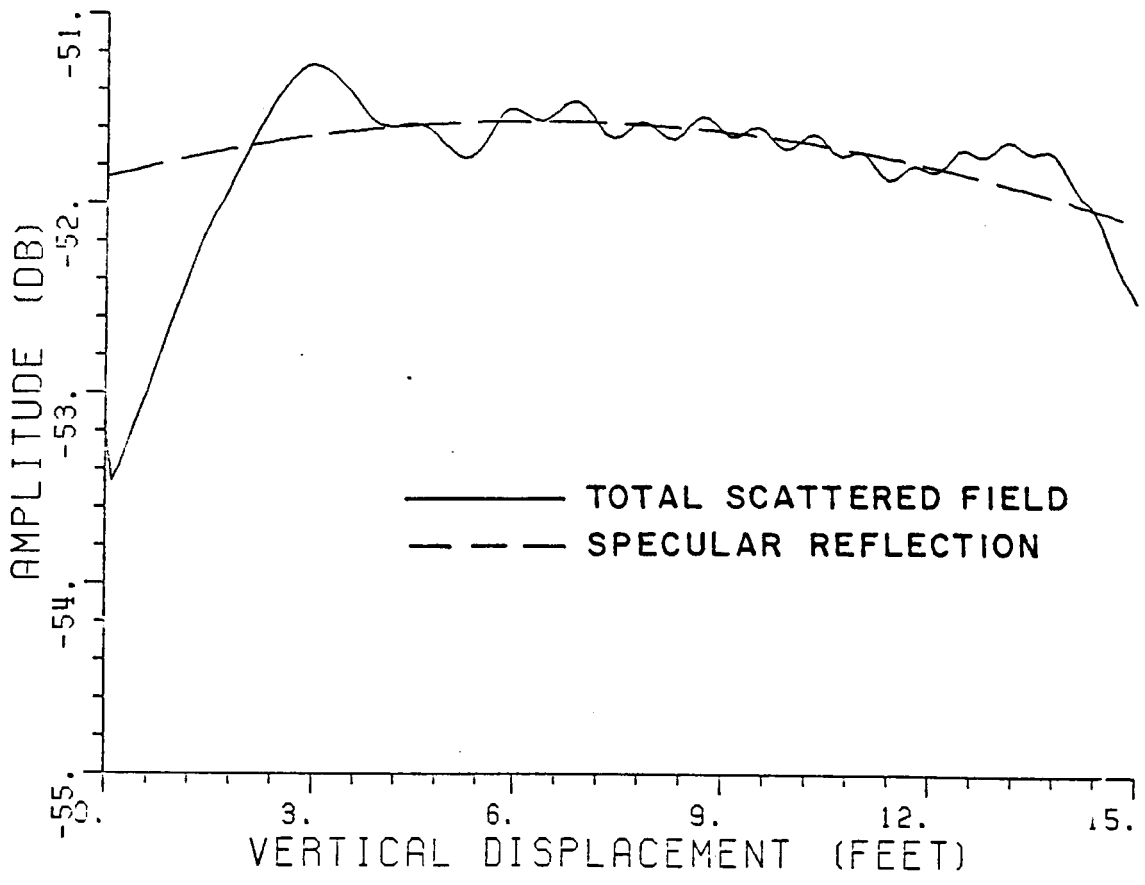

Figure 28. Co-polarized (y) component of the scattered magnetic field versus vertical displacement. Note that ϕ=0°, and the feed is a Huygen's source tilted by 30°. All mechanisms are included in the scattered field.

```
 DO YOU WANT GO TERM?  IF YES, TYPE 1
1
 DO YOU WANT JUNCTION DIFFRACTION?  IF YES TYPE 1
1
 DO YOU WANT SKIRT DIFFRACTION?  IF YES, TYPE 1
1
 DO YOU WANT FEED BLOCKAGE?  IF YES, TYPE 1
1
 DO YOU WANT ELECTRIC FIELD COMPONENTS?  IF YES, TYPE 1
0
 INPUT THE DISTANCE OF THE JUNCTION FROM THE CENTER
 OF THE PARABOLOID IN FEET
15.
 INPUT THE Z LOCATION OF THE FEED APERTURE IN FEET
24.
 INPUT THE NUMBER OF CORNERS IN FEED APERTURE
4
 INPUT THE X,Y COORDINATES OF THE CORNERS IN INCHES
1.5,1.5,-1.5,1.5,-1.5,-1.5,1.5,-1.5
```

The specular reflected component alone is also plotted in Figure 28 (broken curve). Note that for vertical displacements between 3.5 feet and 13.5 feet, the specularly reflected field is quite uniform, and the size of the ripple of the oscillation in the total field is less than 0.2 dB. Thus, the reflector provides a large sweet spot in the vertical dimension.

In the above study, the discussion was limited to the vertical cut (ϕ=0°). To complete the study, the scattered field in other radial cuts is computed next. The discussion is limited to positive values of ϕ. For the negative values of ϕ, the performance will be the same as for the positive values of ϕ. Figure 29 shows the total scattered field for a ϕ=15° radial cut. The other parameters are the same as before. The input data set used for this example is given below:

```
 INPUT THE FREQUENCY IN GHz.
2
 INPUT THE DISTANCE OF THE FOCAL POINT FROM THE
 CENTER OF THE PARABOLOID IN FEET
24.
```

```
 INPUT THE TILT ANGLE OF THE FEED
30.
 INPUT THE MAGNITUDE OF THE MAGNETIC DIPOLES
 ALONG X AND Y AXES
0.,1.
 INPUT THE MAGNITUDE OF THE ELECTRIC DIPOLES
 ALONG X AND Y AXES
1.,0.
 INPUT THE DISTANCE OF THE FIELD PLANE FROM THE CENTER
 OF THE PARABOLOID IN FEET
36.
 INPUT THE PHI CUT IN DEGREES
15.
 INPUT START POINT AND END POINT FOR FIELD PROBING
0.,15.
 INPUT THE DISTANCE BETWEEN FIELD POINTS IN FEET
0.1
 DO YOU WANT GO TERM?  IF YES, TYPE 1
1
 DO YOU WANT JUNCTION DIFFRACTION?  IF YES, TYPE 1
1
 DO YOU WANT SKIRT DIFFRACTION?  IF YES, TYPE 1
1
 DO YOU WANT FEED BLOCKAGE?  IF YES, TYPE 1
1
 DO YOU WANT ELECTRIC FIELD COMPONENTS?  IF YES, TYPE 1
0
 INPUT THE DISTANCE OF THE JUNCTION FROM THE CENTER
 OF THE PARABOLOID IN FEET
15.
 INPUT THE Z LOCATION OF THE FEED APERTURE IN FEET
24.
 INPUT THE NUMBER OF CORNERS IN FEED APERTURE
4
 INPUT THE X,Y COORDINATES OF THE CORNERS IN INCHES
1.5,1.5,-1.5,1.5,-1.5,-1.5,1.5,-1.5
```

Figure 29(a) shows the y (co-polarized) component of the scattered magnetic field while its x component (the cross-polarized component) is plotted in Figure 29(b). The specularly reflected component alone is also plotted in the figure (broken curve). From the plots in Figure 29(a) one can see that the co-polarized component does not vary much for radial displacements between 3.5 feet and 13.5 feet and for

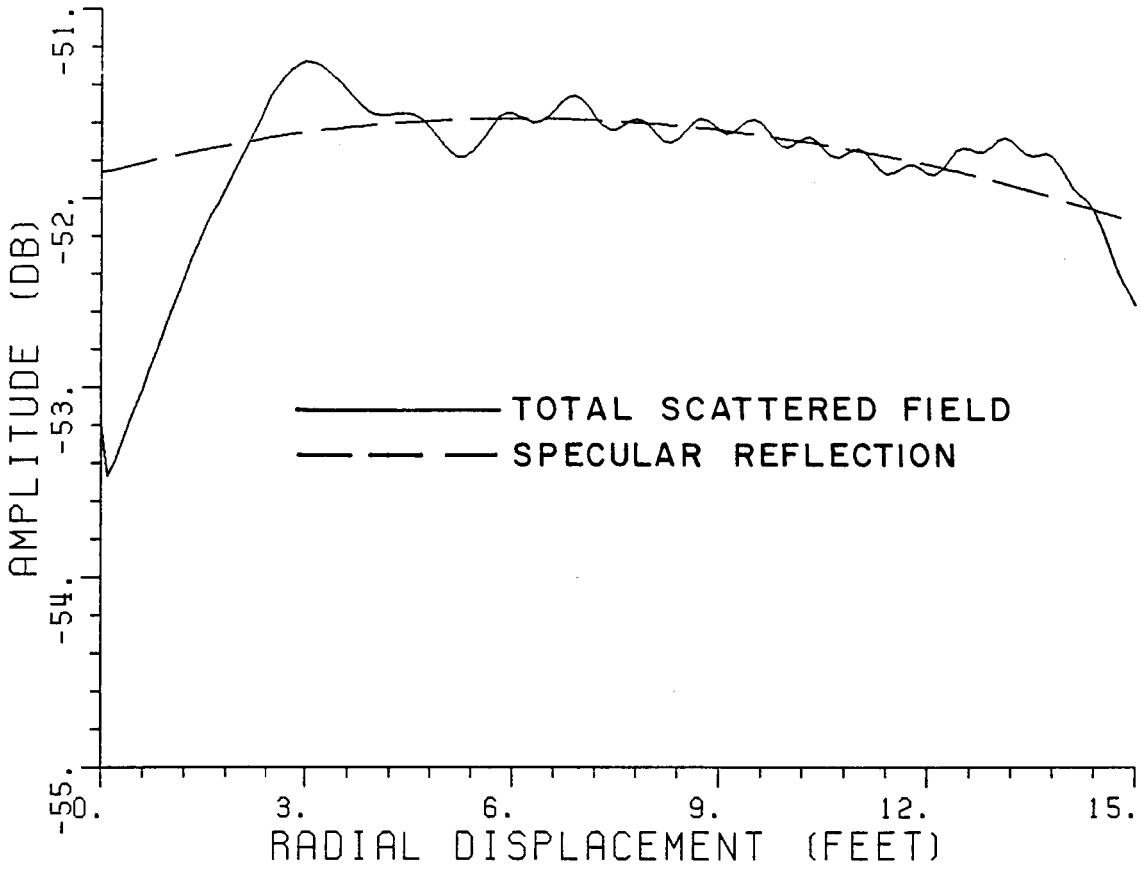

Figure 29(a). Co-polarized (y) component of the scattered magnetic field versus radial displacement. Note that ϕ=15°, and the feed is a Huygen's source tilted by 30°. All mechanisms are included in the scattered field.

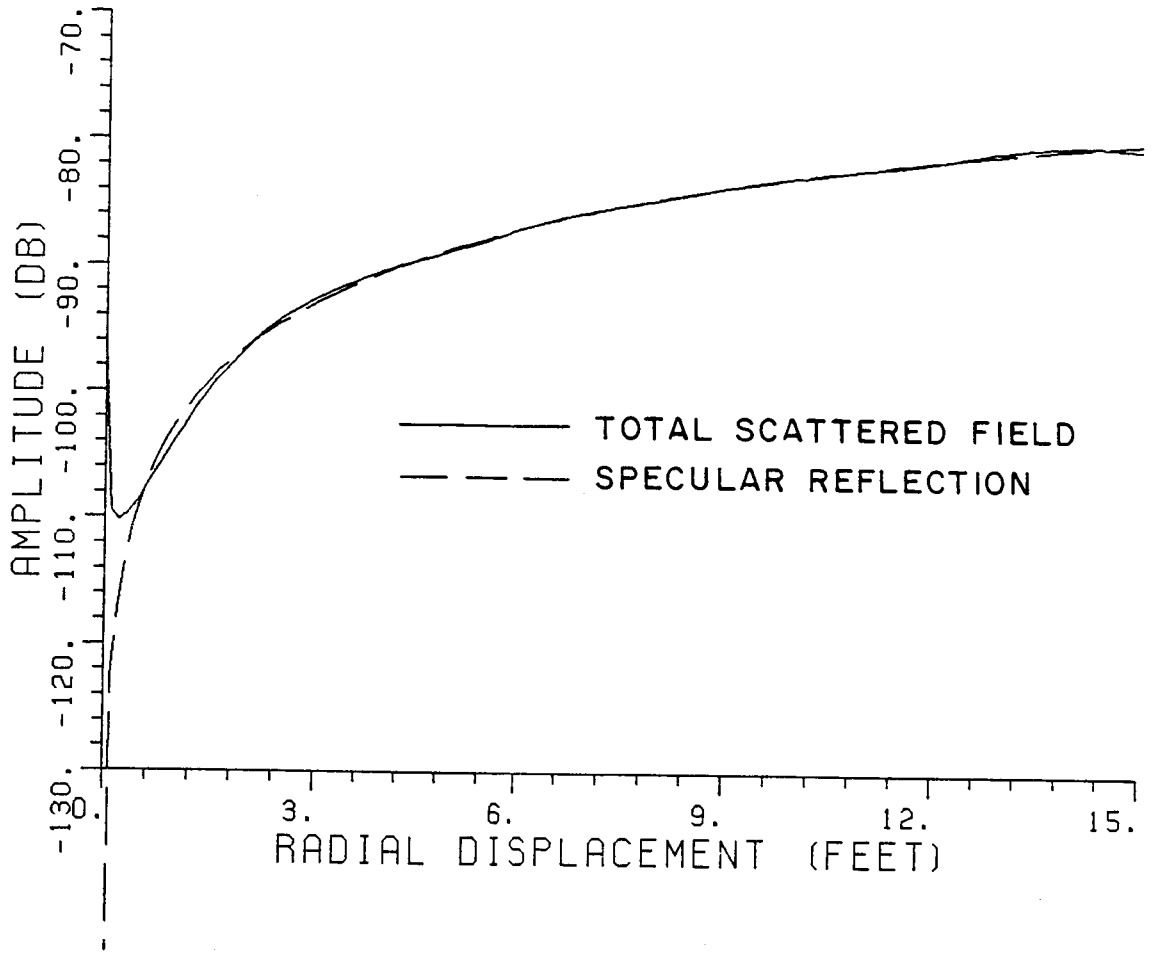

Figure 29(b). Cross-polarized (x) component of the scattered magnetic field versus radial displacement. Note that ϕ=15°, and the feed is a Huygen's source tilted by 30°. All mechanisms are included in the scattered field.

these radial displacements the ripple size of the oscillations is less than 0.2 dB. Thus, one can draw the same conclusions as before. However, in this case the cross polarized scattered field is only 30 dB below the co-polarized component. This may be of some concern in certain applications.

Figures 30, 31, 32 and 33 show the total scattered field for radial cuts of ϕ equal to 30°, 45°, 60° and 75°, respectively. All other parameters are the same as before. Both co-polarized and cross-polarized components of the scattered magnetic field are plotted. The specularly reflected component alone is also plotted (broken curve). Note that the cross-polarized component (x component) of the scattered field has grown. For radial cuts of 45°, 60° and 75°, it is within 17 to 18 dB of the co-polarized component. This may not be desirable. A method of reducing the cross-polarization will be discussed next. However, before that another aspect of these plots will be discussed.

An important observation to be made from the plots of Figures 30-33 is that the length of the radial displacements over which the ripple size of the oscillations is less than 0.2 dB decreases with an increase in the radial cut angle (ϕ). For example, for the 45° radial cut (see Figure 31(a)), the radial displacement for which the ripple size is less than 0.2 dB lies between 5 feet and 13.5 feet while for 60° radial cut (see Figure 32) the radial displacement lies between 7.4 feet and 13.5 feet. For the ϕ=0° radial cut (see Figure 28), the radial displacement for which the ripple size is less than 0.2 dB lies between 3.5 feet and 13.5 feet. Thus, the usable target zone near the axis of the reflector

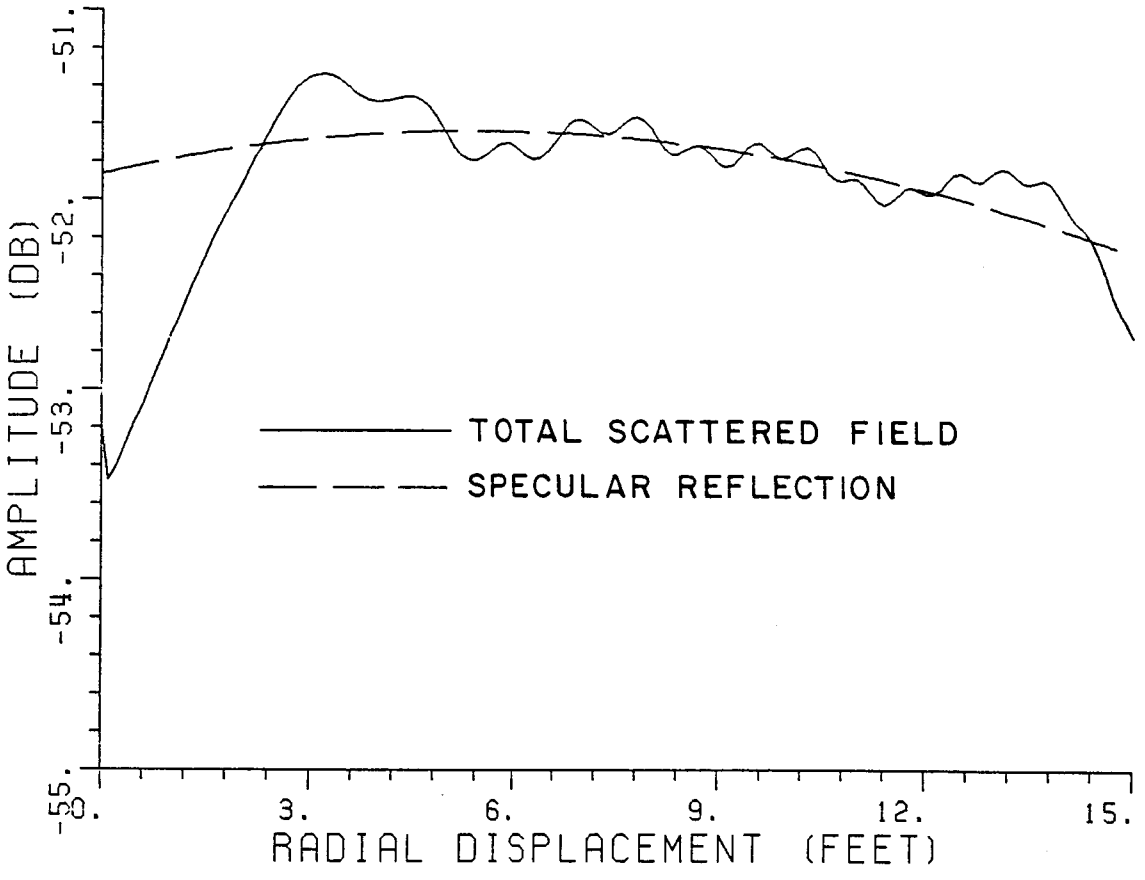

Figure 30(a). Co-polarized (y) component of the scattered magnetic field. Note that $\phi=30°$, and other parameters are the same as in Figure 29(a).

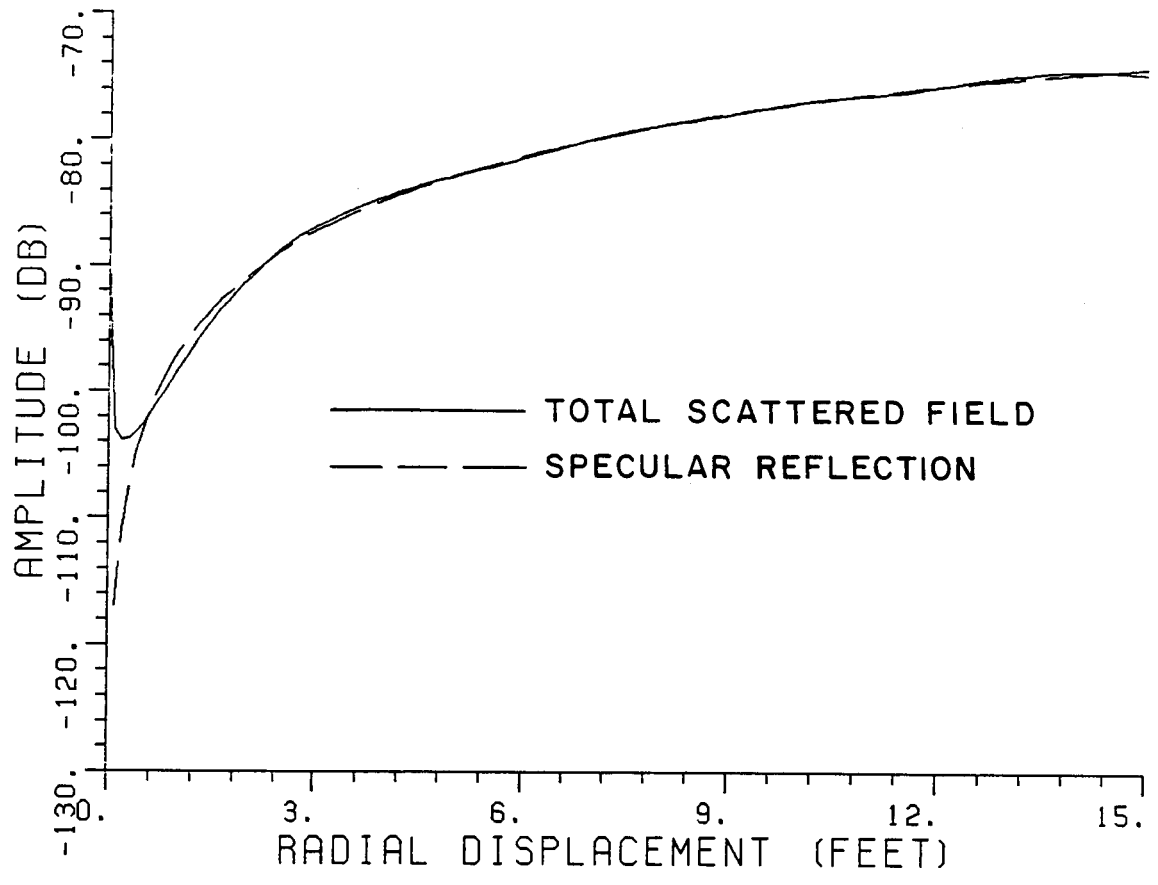

Figure 30(b). Cross-polarized (x) component of the scattered magnetic field. Note that ϕ=30°, and other parameters are the same as in Figure 29(b).

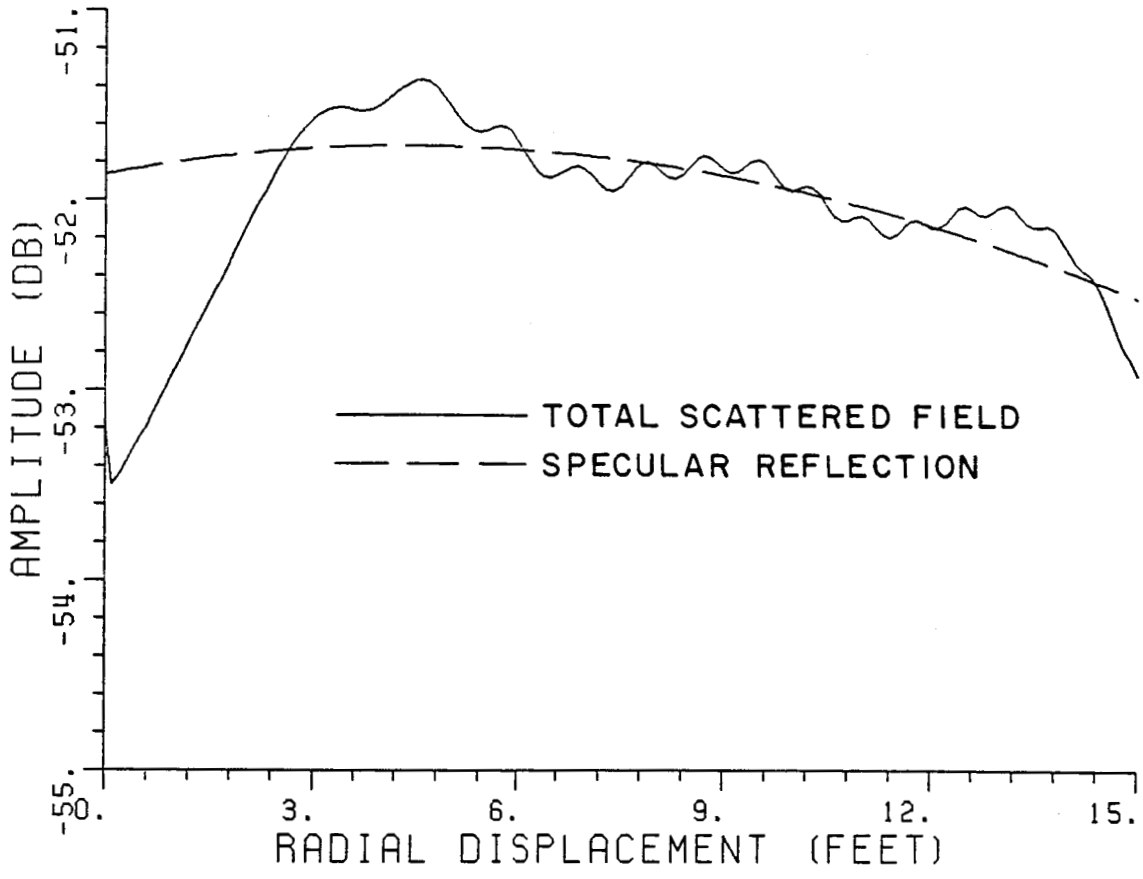

Figure 31(a). Co-polarized (y) component of the scattered magnetic field. Note that ϕ=45°, and other parameters are the same as in Figure 29(a).

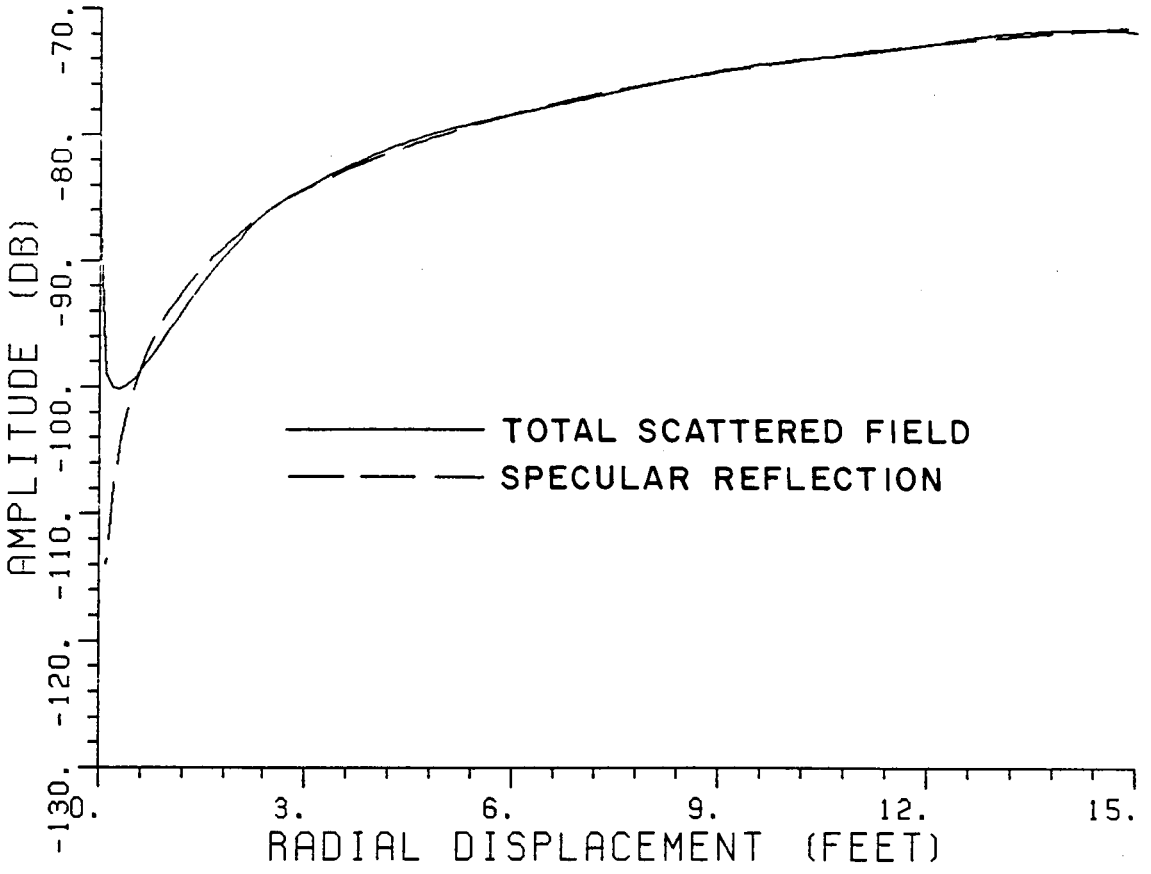

Figure 31(b). Cross-polarized (x) component of the scattered magnetic field. Note that ϕ=45°, and other parameters are the same as in Figure 29(b).

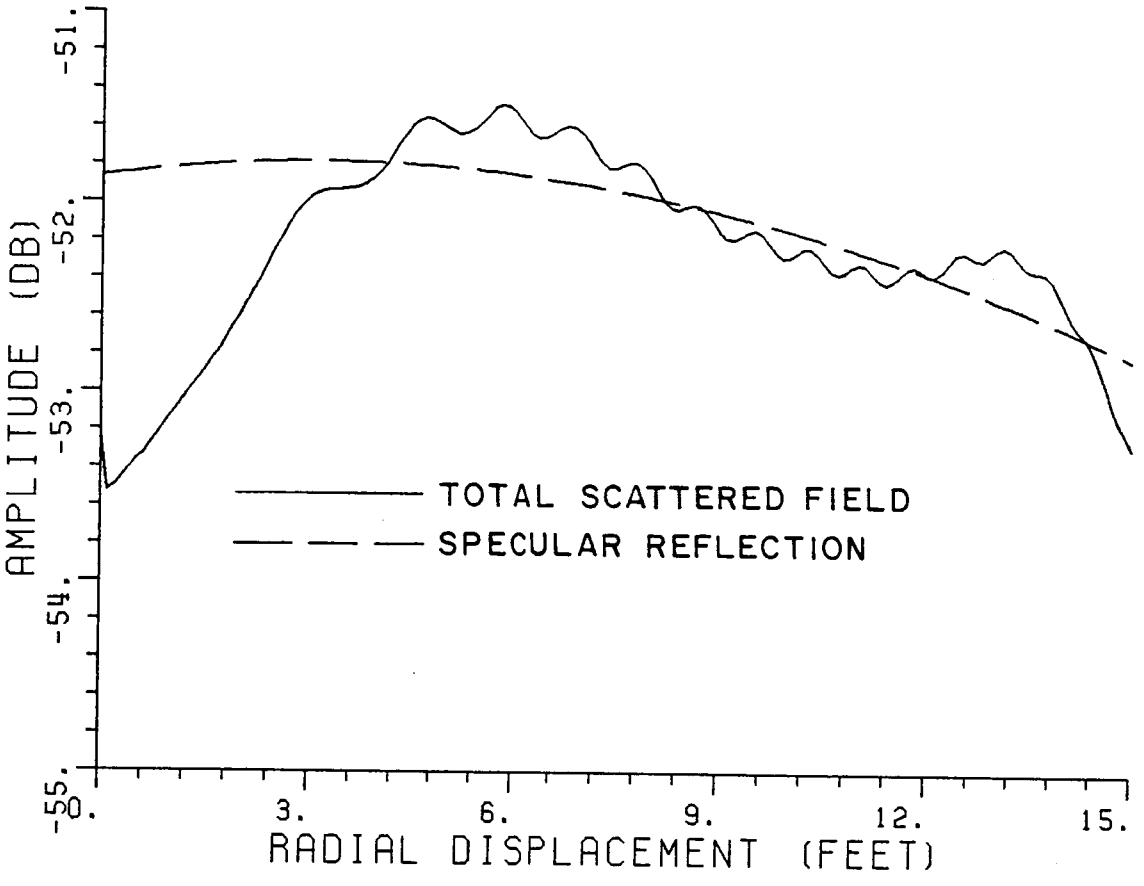

Figure 32(a). Co-polarized (y) component of the scattered magnetic field. Note that ϕ=60° and other parameters are the same as in Figure 29(a).

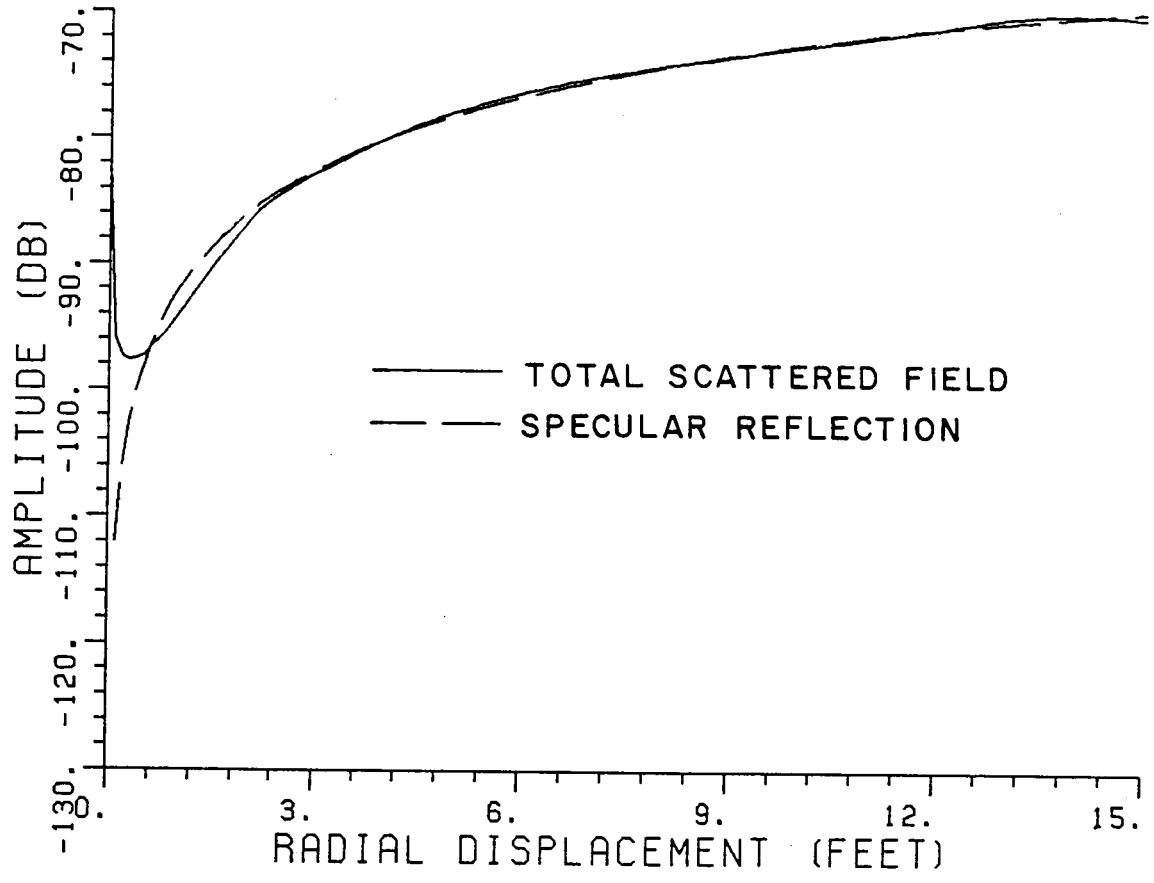

Figure 32(b). Cross-polarized (x) component of the scattered magnetic field. Note that ϕ=60° and other parameters are the same as in Figure 29(b).

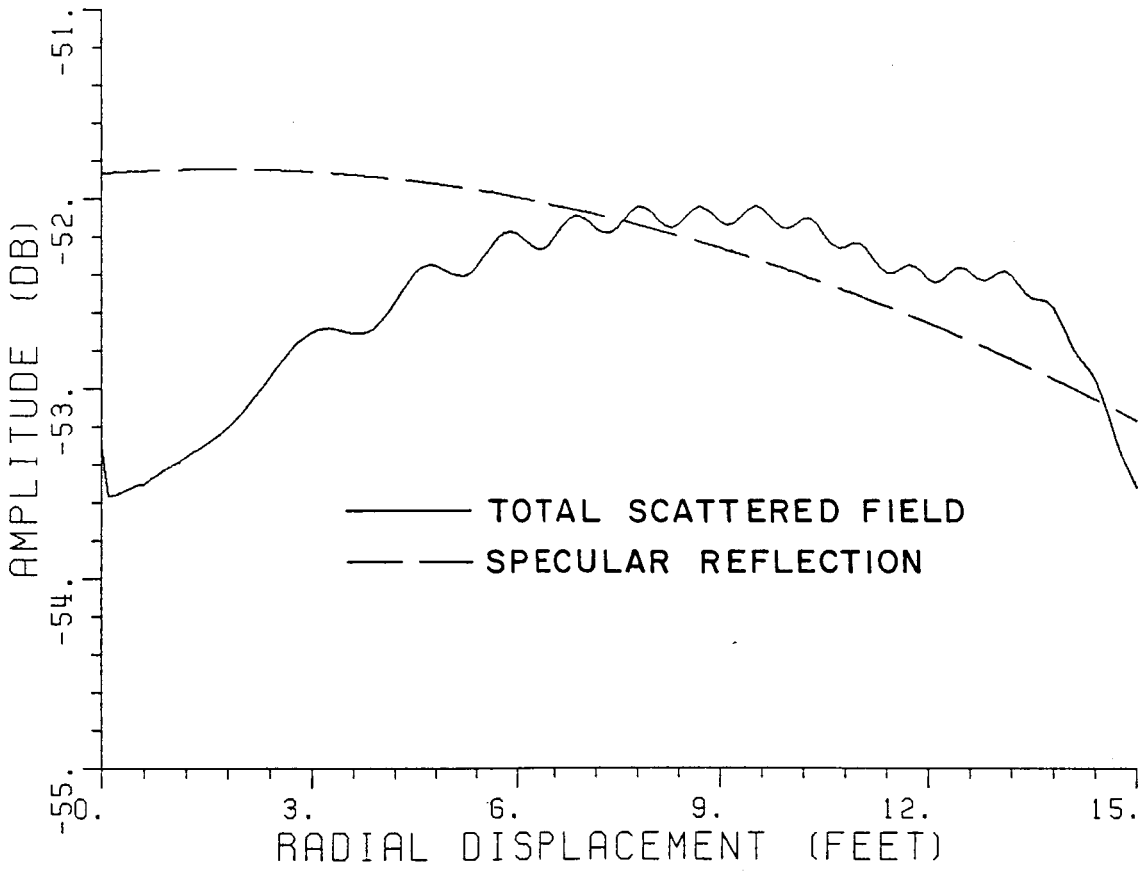

Figure 33(a). Co-polarized (y) component of the scattered magnetic field. Note that ϕ=75°, and other parameters are the same as in Figure 29(a).

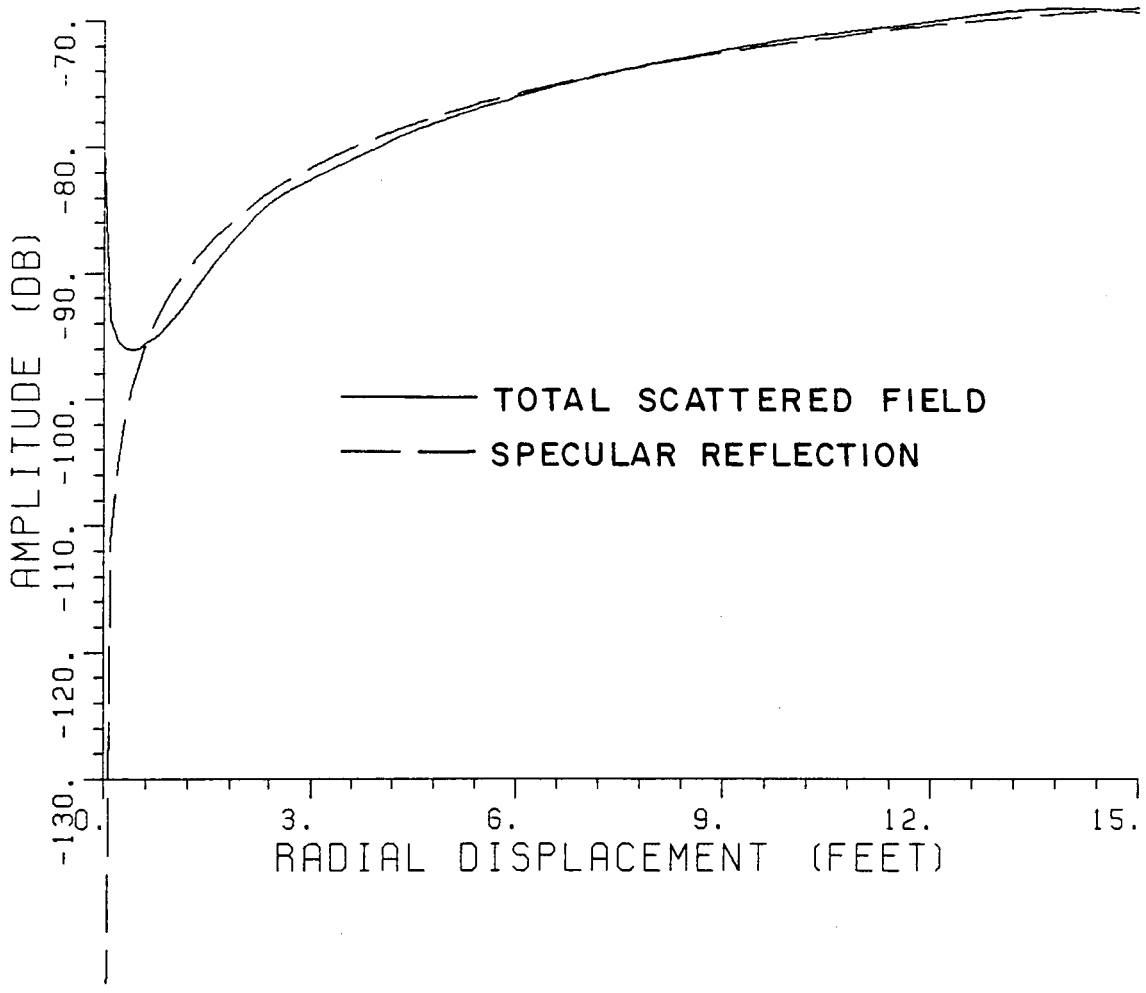

Figure 33(b). Cross-polarized (x) component of the scattered magnetic field. Note that ϕ=75°, and other parameters are the same as in Figure 29(b).

has decreased. The reason for this is that as ϕ increases, the observation point moves closer to the skirt of the reflector, and thus the skirt diffraction becomes a dominant component of the fields in the target zone and limits the size of the usable target zone. This, however, is not a serious problem because this area is not intented to be a part of the target zone. Using this data to define the useable target zone, it (the target zone) looks as shown in Figure 34. Note that the size of the usable target zone is quite large.

Coming back to the cross-polarization issue, one can see from the plots in Figures 29-33 that the specular reflection component is the main contributor to the cross-polarized scattered field. The specular reflection depends on the aperture illumination. Therefore, the aperture illumination should be modified to control the cross-polarized scattered field. One way to modify the aperture illumination is to change the tilt angle of the feed. The effect of the tilt angle of the feed on cross-polarized field is studied next. For the purpose of illustration, the 60° radial cut is chosen to study the effect of tilt angle. In this cut, the cross-polarized scattered field (Figure 32) is quite strong. Since the cross-polarized field is mainly due to the specular reflection, only the specularly reflected component will be computed.

Figure 35 shows the co-polarized and cross-polarized components of the reflected field in the 60° radial cut versus the radial displacement when the tilt angle of the feed is reduced to 25°. All other parameters are the same as before. The input data set is given below:

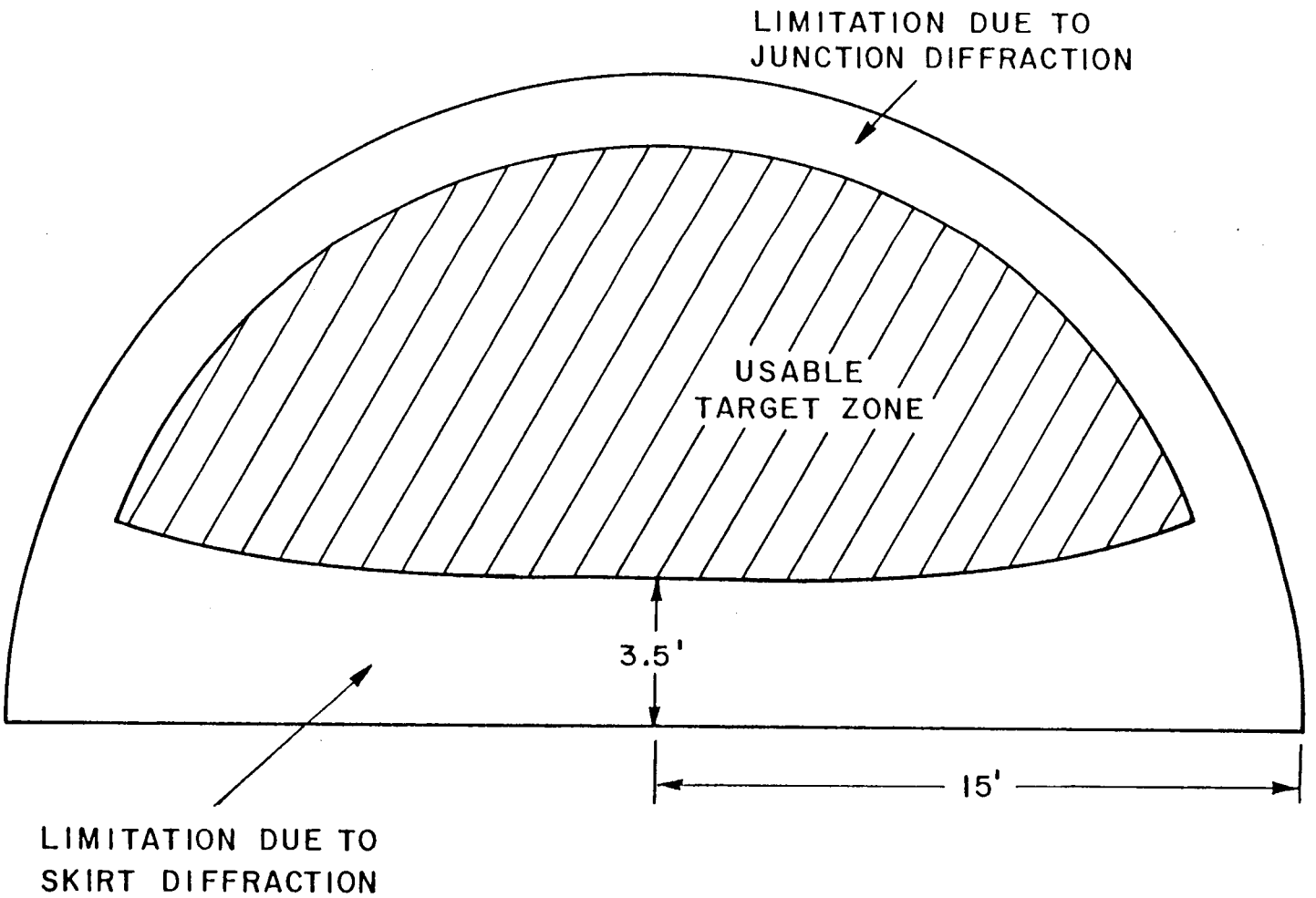

Figure 34. Usable target zone at 2 GHz. Target distance is 36 feet, maximum ripple is 0.2 dB, scale 1" = 4'.

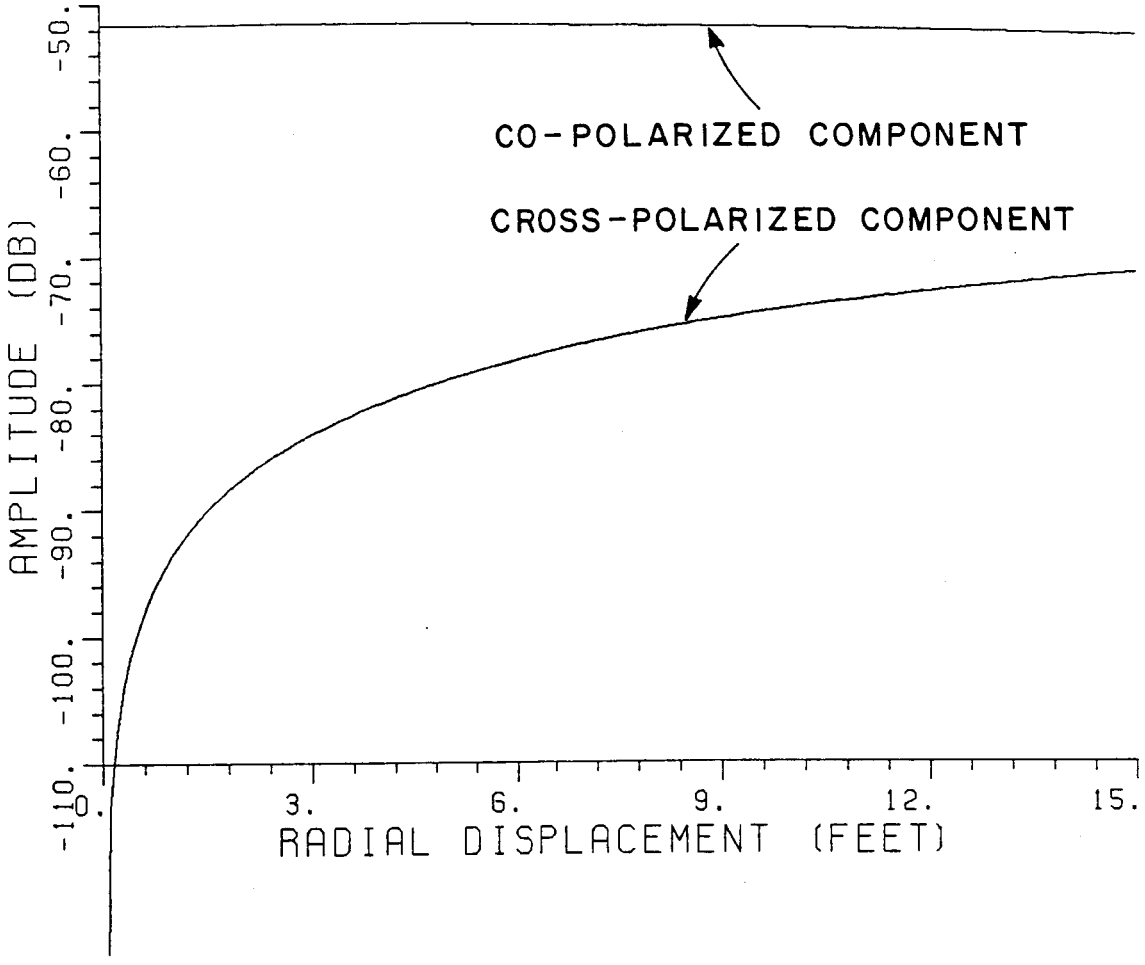

Figure 35. Specularly reflected magnetic field versus radial displacement. Note that ϕ=60°, and the feed is a Huygen's source tilted by 25°.

```
 INPUT THE FREQUENCY IN GHz.
2.
 INPUT THE DISTANCE OF THE FOCAL POINT FROM THE
 CENTER OF THE PARABOLOID IN FEET
24.
 INPUT THE TILT ANGLE OF THE FEED
25.
 INPUT THE MAGNITUDE OF THE MAGNETIC DIPOLES
 ALONG X AND Y AXES
0.,1.
 INPUT THE MAGNITUDE OF THE ELECTRIC DIPOLES
 ALONG X AND Y AXES
1.,0.
 INPUT THE DISTANCE OF THE FIELD PLANE FROM THE CENTER
 OF THE PARABOLOID IN FEET
36.
 INPUT THE PHI CUT IN DEGREES
60.
 INPUT START POINT AND END POINT FOR FIELD PROBING
0.,15.
 INPUT THE DISTANCE BETWEEN FIELD POINTS IN FEET
0.1
 DO YOU WANT GO TERM?  IF YES, TYPE 1
1
 DO YOU WANT JUNCTION DIFFRACTION?  IF YES TYPE 1
0
 DO YOU WANT SKIRT DIFFRACTION?  IF YES, TYPE 1
0
 DO YOU WANT FEED BLOCKAGE?  IF YES, TYPE 1
0
 DO YOU WANT ELECTRIC FIELD COMPONENTS?  IF YES, TYPE 1
0
```

Note that only specular reflection is included in the scattered fields. Comparing the plots in Figures 32 and 35, one can see that the magnitude of the cross-polarized field has dropped by more than a dB. However, even now the cross-polarized component is within 20 dB of the co-polarized component. Thus, the tilt angle of the feed should be further reduced.

Figures 36 and 37 show the co-polarized and the cross-polarized components of the specularly reflected field for feed tilt angles of 15° and 5°, respectively. All other parameters are the same as before. Note that the cross-polarized field decreases with a decrease in the

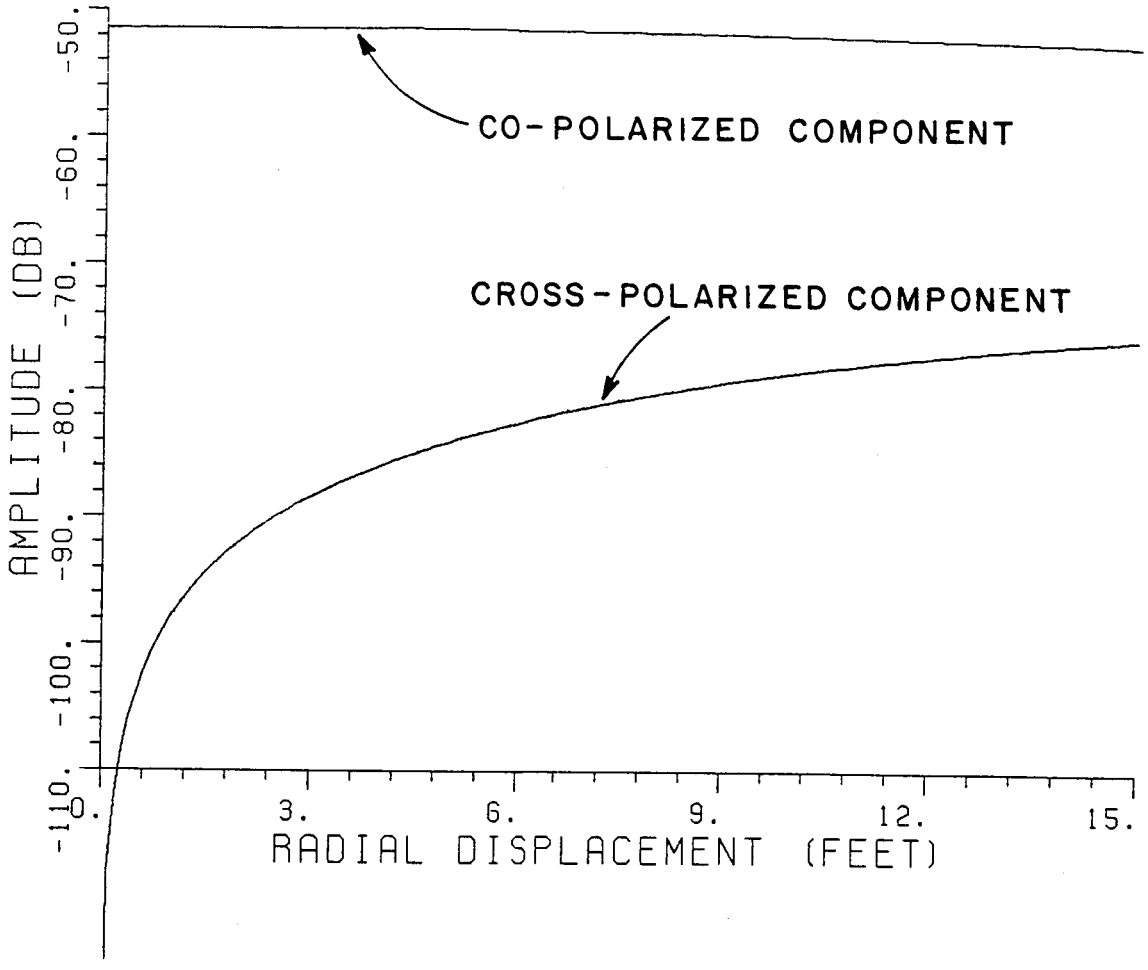

Figure 36. Specularly reflected magnetic field versus radial displacement. Note that ϕ=60°, and the feed is tilted by 15°.

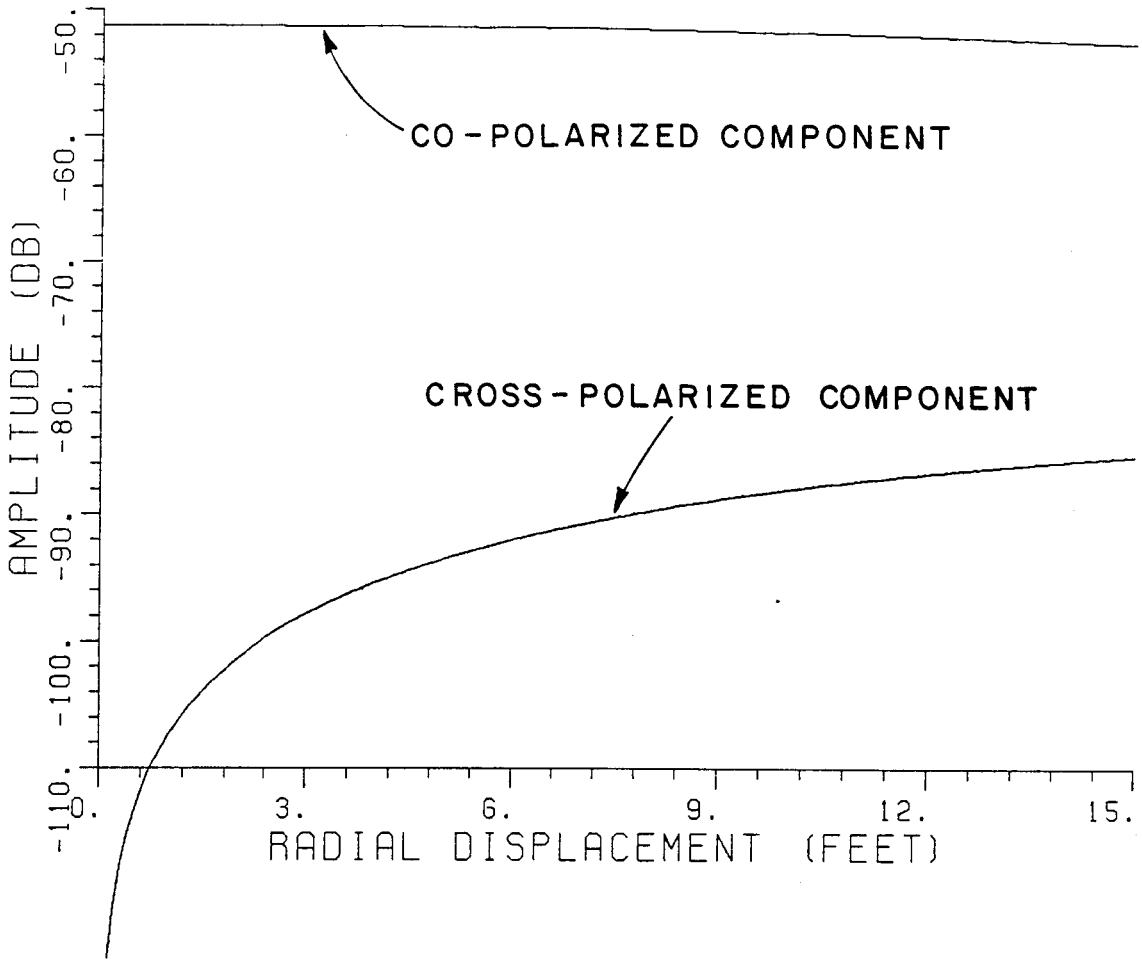

Figure 37. Specularly reflected magnetic field versus radial displacement. Note that ϕ=60°, and the feed is tilted by 5°.

tilt angle of the feed. Thus, by properly selecting the feed tilt angle, the required cross-polarization level can be obtained. Table 1 shows the level of the cross-polarized field with respect to co-polarized field in the 60° radial cut for various tilt angles of the feed. Note that to achieve -40 dB cross-polarization, the tilt angle of the feed should be less than or equal to 2°.

TABLE 1

FEED TILT ANGLE VERSUS CROSS-POLARIZATION

Feed Tilt Angle	Cross-polarization Level
0°	-140 dB
2°	- 40.5 dB
5°	- 32.6 dB
10°	- 28.6 dB
15°	- 23.1 dB
20°	- 20.6 dB
25°	- 18.7 dB
30°	- 17.1 dB

From the above discussion it is clear that the feed should have a very small tilt to keep the cross-polarized scattered field below a certain level. On the other hand, one needs to tilt the feed to get a uniform aperture illumination. Thus, the tilt angle of the feed is an important parameter and should be carefully selected.

In this section various results obtained using the newly developed reflector code were presented to illustrate the code's capability and as samples of input/output sets. It was shown that the codes can be efficiently used to analyze semicircular reflector antennas with a rolled edge.

V. SUMMARY

A computer code has been developed at The Ohio State University ElectroScience Laboratory to analyze a semi-circular paraboloid reflector antenna with a rolled edge at the top and a skirt at the bottom. The operation of the code was described in this report. Various input and output statements were explained. Some results obtained using the computer code were presented to illustrate the code's capability as well as being samples of input/output sets.

APPENDIX A

CODE TO GENERATE THE CROSS-SECTIONAL SHAPE

Computer code 'SURFACE' is used to generate the cross-sectional shape of the cylinder. A listing of the computer code is given below:

```
      PARAMETER (Ndim=9001)
      DIMENSION X(Ndim),Y(Ndim)
      REAL NUF,MAJT,MINT
      COMMON /ONE/ FM,NUF,IBLEND
      COMMON /TWO/ YIT,YFT,MAJT,MINT,THETAT,XELT,YELT
C**   -------------------------------------------------
      READ(70,*) FMC         ! frequency in GHz.
      READ(70,*) FM          ! focal distance in feet
      READ(70,*) YIT         ! y coordinate of the upper end of parabola
      READ(70,*) YFB         ! y coordinate of the lower end of parabola
      READ(70,*) IBLEND      ! type of blending (IBLEND = 1, 2, 3 or 4)
      READ(70,*) PSECT       ! length(cms) of the parabolic section blended
      READ(70,*) NUF         ! section of the ellipse blended = 180 deg.
      READ(70,*) MAJT,MINT   ! major and minor axis of ellipse in cms.
      READ(70,*) DSSwl       ! spacing between samples in wavelength.
C**   -------------------------------------------------------
      cdimin  = 30.48006096 ! conversion constant from feet to centimeters
      FM      = cdimin*FM
      YFB     = cdimin*YFB
      YIT     = cdimin*YIT
      DSS     = DSSwl*29.97925/FMC   ! DSS in centimeters
      NUF=NUF*3.141592654/180.
      YFT=YIT+PSECT
      XATYIT=YIT**2/(4.*FM)
      XELT=XATYIT-MINT/SQRT(1.+(YIT/(2.*FM))**2)
      YELT=YIT+MINT*YIT/(2.*FM)/SQRT(1.+(YIT/(2.*FM))**2)
      THETAT=ASIN((XATYIT-XELT)/MINT)
      N=1
C
C PARABOLIC SECTION
C
      PY=YFB
      CALL XYCORM(PY,X(N),Y(N))
40    CONTINUE
      DXDY=Y(N)/(2.*FM)
      DY=DSS/SQRT(1.+DXDY**2)
      N=N+1
      PY=PY+DY
      IF(PY .GE. YIT) GOTO 50
      CALL XYCORM(PY,X(N),Y(N))
      GOTO 40
C
```

```
C UPPER ROLLED EDGE
C
50       PY=YIT
         CALL XYCORM(PY,X(N),Y(N))
60       DXDY=Y(N)*0.5/FM
         DY=DSS/SQRT(1.+DXDY**2)
         PY=PY+DY
         IF(PY .GT. YFT) GOTO 70
         N=N+1
         CALL XYCORM(PY,X(N),Y(N))
         GOTO 60
70       CONTINUE
         WRITE(17,*) N
         DO 100 I=1,N
 100     WRITE(17,*) X(I),Y(I)
         CALL EXIT
         END


C THIS SUBROUTINE CALCULATES THE X AND Y COORDINATES, GIVEN PY
C
         SUBROUTINE XYCORM(PY,X,Y)
         REAL NU,NUF,MAJT,MINT
         COMMON /ONE/ FM,NUF,IBLEND
         COMMON /TWO/ YIT,YFT,MAJT,MINT,THETAT,XELT,YELT
C
         IF (PY.GT.YIT) THEN
            NU=NUF*(PY-YIT)/(YFT-YIT)
            GOTO (12,14,16,18),IBLEND
12          BLEND=0.
            GOTO 20
14          BLEND=1.-NU/NUF
            GOTO 20
16          BLEND=1.-(NU/NUF)**2
            GOTO 20
18          BLEND=(1.+COS(3.141592654*NU/NUF))/2.
20          X=PY**2/(4.*FM)*BLEND+(MAJT*SIN(NU)*
      1     COS(THETAT)+MINT*COS(NU)*SIN(THETAT)+XELT)*(1.-BLEND)
            Y=PY*BLEND+(MAJT*SIN(NU)*SIN(THETAT)-MINT*COS(NU)
      1     *COS(THETAT)+YELT)*(1.-BLEND)
         ELSE
            X=PY**2/(4.*FM)
            Y=PY
         ENDIF
         RETURN
         END
```

The code reads the input data from unit #70. Various parameters read by the code are shown between dashed lines in the code and are self explanatory. To further help the user, the various parameters are shown in Figure 38. IBLEND in the input data defines the blending between the parabolic and elliptical sections. IBLEND is equal to 1, 2, 3 or 4 for

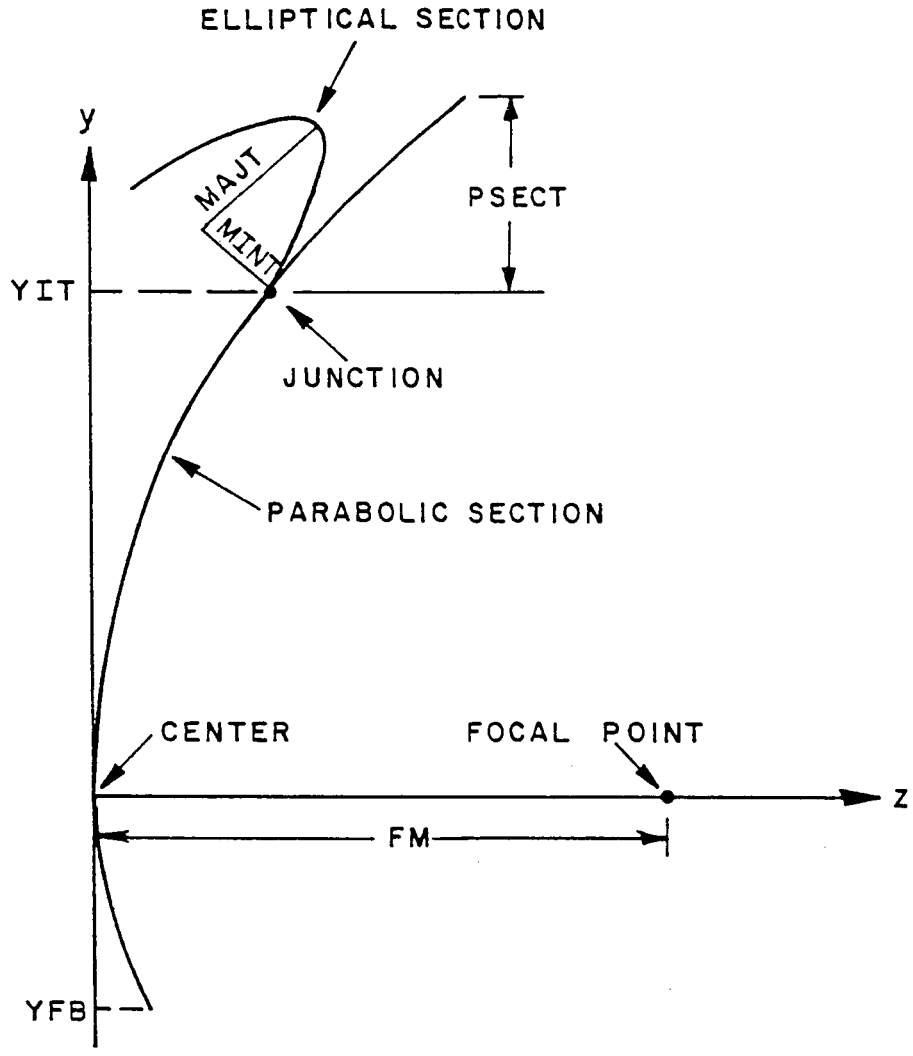

Figure 38. Various parameters used in the code.

no blending, linear blending, square blending and cosine blending, respectively. The blended section is defined as follows.

$$x = x_p(\nu)B(\nu) + x_e(\nu)[1-B(\nu)]$$

and

$$y = y_p(\nu)B(\nu) + y_e(\nu)[1-B(\nu)]$$

where (x_p,y_p) and (x_e,y_e) are the coordinates of the point on the parabola and the ellipse, respectively. Note that B is the blending function which is defined by

$$B(\nu) = \begin{cases} 0 & \text{no blending} \\ 1-\nu/\nu_f & \text{linear blending} \\ 1-(\nu/\nu_f)^2 & \text{square blending} \\ \dfrac{1+\cos\left(\frac{\pi\nu}{\nu_f}\right)}{2} & \text{cosing blending} \end{cases}$$

where ν_f(NUF) is an input parameter and is normally set equal to 180°.

DSSωℓ in the input data is the spacing between adjacent samples in wavelengths and should be of the order of 0.05 wavelength. The code in its present form can store up to 9001 samples. If the number of samples on the cross-sectional shape exceeds 9001, the first statement in the code should be adjusted accordingly.

REFERENCES

[1] R.G. Kouyoumjian and P.H. Pathak, "A Uniform Geometrical Theory of Diffraction for an Edge in Perfectly Conducting Surfaces", Proc. of IEEE, pp. 1448-1461, November 1974.

[2] Tai-Tseng Chu, "First Order Uniform Geometrical Theory of Diffraction Analysis of Scattering by Smooth Surfaces", Ph.D. Dissertation, The Ohio State University, Department of Electrical Engineering, Columbus, Ohio, March 1983.

[3] W.B. Gordon, "Far-Field Approximations to the Kirchoff-Helmholtz Representations of Scattered Fields", IEEE Transactions on Antennas and Propagation, Vol. AP-28, No. 4, pp. 590-592, July 1975.